https://doi.org/10.5194/egusphere-2026-2864
Preprint. Discussion started: 4 June 2026

Microbial Interactions with Dissolved Organic Matter (DOM) from Immature Cretaceous Marine Black Shale: *Implications for subsurface carbon flux and geothermal energy systems*

Muhammad S. Jibrin[1,2], Abdulhamid Dahiru[3]

[1]Department of Pure and Industrial Chemistry, Bayero University, Kano, 700241, Nigeria.

[2]Lyell Centre, Heriot-Watt University, EH14 4AS, UK

[3]Lipid Technology Laboratory, School of Bioresources and Technology, King Mongkut's University of Technology Thonburi, Bangkhunthian, Bangkok, 10150, Thailand

Correspondence to: Muhammad S. Jibrin (msjibrin.chm@buk.edu.ng)

Abstract

Microbial transformation of dissolved organic matter (DOM) is a central process in subsurface carbon cycling, yet its long-term dynamics in shale environments remain poorly constrained. We conducted an 810-day incubation experiment using DOM leached from immature Cretaceous marine black shale to investigate fluid–rock–microbe interactions and their role in climate-active gas generation. Liquid chromatography–organic carbon detection (LC-OCD) revealed progressive microbial degradation of labile DOM pools and the accumulation of recalcitrant fractions, accompanied by sustained CO_2 and CH_4 release. These findings demonstrate that shale DOM can fuel persistent microbial metabolism, restructure DOM composition, and contribute to subsurface carbon fluxes over extended timescales. Our results highlight the ecological significance of shale DOM biodegradation in unlocking deep carbon reservoirs and provide new insights into the microbial mediation of subsurface biogeochemical cycles.

1.0 Introduction

The biogeochemical degradation and transformation of dissolved organic matter (DOM) are critical for its contributions to the global carbon (C) cycle and the C flux in ecosystems (Schlesinger and Andrews, 2000; Davidson and Janssens, 2006; Heimann and Reichstein, 2008). Microorganisms are important intermediaries in the formation, mobilisation, transformation, mineralisation, and storage of DOM in various environments, such as shale, soil, sediment, and marine and freshwater (Ji et al., 2023; Young et al., 2004; Jiao et al., 2010; Lin et al., 2014; Zhuet al., 2016; Wu et al., 2018; Spray et al., 2021). Understanding the dynamic interactions among substrate/rock, DOM, and microbial activities is critical not only to delineate the routes of DOM mobilisation, transformation, and flux in the surface and subsurface environments but also to determine the release of climate-active gases (CO_2 and CH_4) from these processes. Identifying DOM groups accessible to microbial activity and understanding microbial transformation and mineralisation of DOM are central to this challenge. However, these processes and interactions

https://doi.org/10.5194/egusphere-2026-2864
Preprint. Discussion started: 4 June 2026

in natural and engineered subsurface environments are commonly studied independently (Wu et al., 2018) and so lack a comprehensive and integrated understanding. This knowledge is pressing as drilling activities for geothermal and unconventional energy using hydraulic fracturing are increasing globally (Mouser et al. 2016), and are likely to stimulate biophysical-chemical perturbations in the deep subsurface, with unknown consequences. A key component in this process is the injection of fluids into the sub-surface, which are not sterile (Mouser et al. 2016). Thereby, surface microbes and chemicals can be introduced into the subsurface while (re-)activating subsurface microbial communities that can exist up to 3–5 km in the deep subsurface (Kadnikov et al., 2020). It is therefore possible, if not likely, that highly pressurised injection fluids mobilise natural organic matter and other inorganic nutrients from the sub-surface rock, thereby creating a complex mixture of in situ (autochthonous) and surface (allochthonous) DOM, mineral, and microbial communities that can interact with sub-surface fluid flow. This autochthonous source of DOM may be more biologically available, despite its lower concentration compared to the larger and possibly more stable allochthonous DOM (Findlay and Parr, 2017). Consequences for engineering are well known and include biogenic CO_2/CH_4 generation, reservoir/borehole souring leading to corrosion of the installed facilities, biofilm formation from rapid microbial bloom growth, which may constrain fluid flow, as well as borehole fouling (Ren et al., 2024; Vetter et al., 2012). This study aims to investigate whether the leached aged OM from a subsurface rock could stimulate microbial activity leading to GHG generation.

The deep subsurface hosts a large and diverse microbial community (Mouser et al., 2016). Pioneering works in mines, boreholes/wells, and springs have confirmed that the deep subsurface is a habitable setting rather than vast expanses of sterile rock (Colwell and D'Hondt, 2013). The deep terrestrial (or continental) biosphere is structurally complex, resulting in heterogeneous geological environments (Osburn et al., 2020). These environments and geological gradients with their unique microbial habitats and sources of energy and carbon (such as DOM) are modified by hydrological connectivity in aquifers, or, for engineering operations, fractured- (or drilled-) based mixing (Osburn et al., 2020). Large open questions remain relating to the stability and connectivity of these in-situ (subsurface) and introduced-terrestrial microbial taxa, a plethora of complex DOM (both autochthonous and allochthonous), their resultant interactions in the sub-surface, and their engineered and natural connectivity with the surface.

To understand these sub-surface processes and interactions, the UK government initiated the United Kingdom Geoenergy Observatory Site Project (UKGEOS) to explore the deep subsurface environment for geothermal energy production as part of its strategy towards decarbonisation of energy by 2050 (HM Government, 2021). Geothermal energy is a promising alternative energy source that may allow for faster, wider, and more efficient cleaner energy (EU (CORDIS), 2020).

https://doi.org/10.5194/egusphere-2026-2864
Preprint. Discussion started: 4 June 2026

However, the process of deep energy extraction involves perturbation of the deep subsurface, which may mobilise bedrock carbon and other elements (including nutrients and metals) and introduce or reactivate microbial taxa in the subsurface. These processes may potentially stimulate microbial activities producing greenhouse gases (GHG) in the sub-surface and leakage to the surface environment (Fig 1). These DOM-microbial interactions might also pose challenges to the exploitation and operation of geothermal boreholes by altering the chemical properties of the fluids through biodegradation products, corrosion, and pipeline clogging, leading to well fouling (Leins et al. 2022). Hence, it is critical to document and understand these deep subsurface interactions to de-risk geothermal energy production.

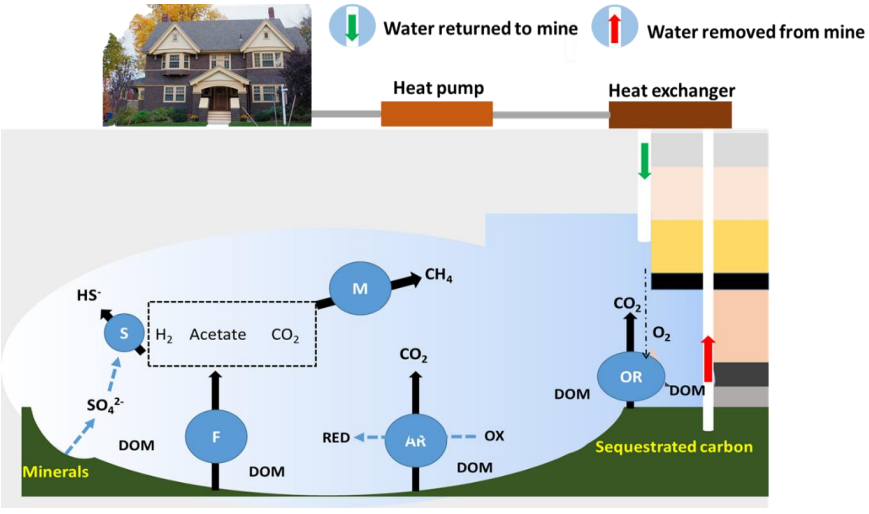

Figure 1: An ecological model of the deep subsurface aquifer for geothermal energy production, indicating the inflow and outflow of cold and hot water, resulting in the mobilisation and deposition of DOM due to temperature and pH differences, the introduction of O2, and the mobilisation of sequestrated C substrates and mineral nutrients, which may support microbial activity. Key: OR, aerobic respiration; F, fermentation; SR, sulphate reduction; AR, anaerobic respiration (other than SR); M, methanogenesis. (Modified from Kadnikov et al. 2020). Note: the model does not represent the real dimension/size of the aquifer, but a rather idealised cartoon of engineered mobilised DOM-microbial interactions in the subsurface aquifers and how it influences biogeochemical changes and generation of climate active gases (CO_2/CH_4).

To contribute to these wider challenges, we conducted a set of long-term microcosm experiments using organic-carbon-rich immature Cretaceous source rocks as a substrate to test the potential of geologically old DOM to stimulate microbial activities, before exploring the more complex, OM-rich coal-bearing environment of Carboniferous rock lithologies recorded from the UKGEOS study site. This is critically needed to understand and better predict fluid-rock–microbial interaction in new geothermal systems, and the modelling and operation of such systems.

The DOM chemistry strongly affects the microbial community structure and their metabolic potential, as shown for marine (McCarren et al., 2010), soil (Ding et al., 2015), groundwater

https://doi.org/10.5194/egusphere-2026-2864
Preprint. Discussion started: 4 June 2026

environments (Zhang et al., 2015), and sediment leachates (Wu et al., 2018). Tracing and investigating DOM changes with microbial activity is complex, as the change in microbial community structure and function coupled with the contribution of microbial products (i.e. bacterial lysates released from dead cells, extracellular metabolites, and microbially produced aromatic amino acids e.g., phenylamine, tyrosine, tryptophane) to the DOM pool can affect the transformation of DOM and contribute to changes in DOM composition over time (Goodwin et al., 2015; Turnbull et al., 2016; Wu et al., 2018). These microbially derived products and biodegradation residues are, for example, polysaccharides, proteins, and cell wall polymers, together with several uncharacterized molecules that can become an integral component of OM during the process (Kogel-Knabner, 2002; Kelleher and Simpson, 2006; Koch et al., 2014; Osterholz et al., 2015; Kallenbach et al., 2016). Therefore, the bioavailability of C substrate in DOM, microbial community composition, and the ability of microbes to metabolise DOM are closely interconnected, but such interactions are not well documented for the subsurface environment.

The DOM leached from rocks serves as the main source of C to groundwater (Aiken, 2002) and contributes to the permanent groundwater DOC pool that is decoupled from seasonal shifts in organic C content at shallower depths due to fluid flow and recharge (Awoyemi et al., 2014). The highly pressurised drilling fluids induced by drilling and hydro-fracking facilitate the release of DOM from rocks in the deep subsurface (Vieth-Hillebrand et al., 2017). The DOM signature and function are linked to the kerogen type of the host rock and therefore may interact in different ways with the autochthonous (groundwater/fluid-flow) and allochthonous (drilling fluid) origins of microbial communities in the subsurface (Ding et al., 2015). Investigations that link rock DOM turnover to microbial activities and biogenic CO_2/CH_4 production in subsurface settings are rare (Wu et al., 2018). Therefore, in this study, the surface water microbes were exposed to water-leached DOM from thermally immature Cretaceous marine black shale and biogenic CO_2 and CH_4 production was monitored using a greenhouse gas analyser (GHG) during 810 days of incubation. This approach will account for longer-term interaction effects and thereby significantly extend previous studies (Horstmann, L. (2018); Wu et al., 2018) that focus on shorter (2-month) incubation periods. To document the change in DOM composition before and after our incubations, the LC-OCD was used. This research hypothesised that H1: Water-extracted DOM may stimulate microbial activity and generate GHG. H2: The microbial activity will gradually transform the black shale-derived DOM pool towards more recalcitrant DOM (less labile lipid and lignin-like macro-molecules). H3: The amount and composition of DOM pools directly dictate the amount of GHG (CO_2/CH_4) generated by microbial activity.

https://doi.org/10.5194/egusphere-2026-2864
Preprint. Discussion started: 4 June 2026

2.0 Methodology

2.1 Sample collection

2.1.1 Cretaceous marine black shale sample

Two Cretaceous black shale samples (A and B) were selected from study well S75 at the deep part of the Tarfaya basin in southern Morocco, offshore North-West Africa. See Kolonic et al. (2002) for further details on the location and geochemistry. The stratigraphic section represented in the study interval belongs to the Cenomanian-Turonian transition (upper *Rotalipora cushmani* to middle *H. Helvetica biozone*) of the Oceanic Anoxic Event 2. Samples of 2 and 5 cm thickness were taken for this study. The two samples were selected for the experiment based on their OM richness, kerogen type, and thermal immaturity. Sample A was obtained from 60 cm well depth, while sample B was collected from 120 cm, both representing high TOC palaeo-shelf marine environments (Kuhnt et al., 1990; 1997). In this study, we used elemental and Rock-Eval pyrolysis data obtained by Kolonic et al. (2002). The total organic carbon content of samples A and B is 7.5 and 10.5 (w %), respectively. The OM in the samples is thermally immature (Tmax; 411 °C and 407 °C, respectively) with pyrolytic kerogen yields (S2) of 55.23 and 83.3 mg HC/g rock, respectively. Both samples have very high Hydrogen Indices (HI; 733 and 795 mg HC/g TOC, respectively) and low Oxygen Index (OI; 53 and 43 mg CO_2/g TOC, respectively), qualifying the kerogen as marine/microbial type I to IIs.

2.1.2 Inoculum – Freshwater sample

The microbial community used as inoculum for the microcosm experiment of this study was obtained from the Black Burn River, Auchencorth Moss field, located in Southeast Scotland (55°48'21.5" N; 3°13'36.0" W). The catchment has a long-term data set relating both terrestrial and aquatic carbon species, which includes a complete, inter-annual C and GHG budget from 2008 onwards (Dinsmore et al. 2010). The vegetation that covers the main body of the peatland consists of grasses, rushes, and sedges (Drewer et al. 2010). The peat catchment is drained by the Black Burn, a small stream with a width of ~1 m and a depth from peat surface to channel bed of ~1.2 m. The Burn River is characterised by low pH (~3-6), low-temperature conditions, and a dynamic hydrological response to rainfall events (Billett and Harvey, 2013; Dinsmore and Billett, 2008). Stream water is commonly highly coloured and mean long-term DOC concentrations are 28.4 ± 1.07 mg L^{-1} (Dinsmore et al. 2013).

The freshwater sample was obtained in a 10 L High-Density Polyethylene (HDPE) carboy one day before incubation and stored at room temperature. The carboy and 1L HDPE wide-neck bottle were pre-cleaned with 18.2 MΩ cm^{-1} decarbonised water before the sampling. Both the carboy and bottle were rinsed three times with river freshwater before sampling and were sampled from

https://doi.org/10.5194/egusphere-2026-2864
Preprint. Discussion started: 4 June 2026

mid to the bottom of the river (the soil from the bottom of the river was also collected with the water sample).

2.2 Extraction of DOM from the Cretaceous shale samples

The PTFE bottles (50 mL) used for leaching of the shale samples were pre-cleaned by soaking in a 10% HCl/18.2 M Ωcm^{-1} water (v/v) for 30 minutes, transferred to an 18.2 M Ωcm^{-1} water bath, and then rinsed with 18.2 M Ωcm^{-1} water and dried up on a drying rag covered with ashed aluminium foil. The ground shale samples (A and B; three 3g each) were measured into pre-cleaned Teflon tubes, and 37.5 mL 18.2 MΩ cm^{-1} decarbonised water (1:12.5 wt./v) was added and placed in a shaking incubator, at a temperature of 50 °C for 48 hours (Zhu et al. 2015). The samples were filtered with GF/F membrane filters, diameter 70 mm, pore size 0.7 µm (Whatman) in a 250 ml glass bottle and rinsed with an additional 50 mL 18.2 MΩ cm^{-1} decarbonised water. The samples were immediately re-filtered using a Polyether sulfone (PES) filter 0.45 µm for injection to LC–OCD, which is suitable for DOM analysis (Karanfil et al., 2002). The resulting filtrates were analysed using LC-OCD (according to Huber et al. (2011) and Zhu et al (2015)) to identify different DOM fractions. The post-incubation inoculum samples were also filtered with a 0.45 µm PES filter before LC-OCD analyses to determine the biotransformation of DOM at the end of the incubation.

2.3 Incubation of surface water microbes with black shale-derived DOM

2.3.1 Pre-incubation preparation

The microcosms were set up in 100 mL glass serum bottles. All the bottles were cleaned and rinsed with 18.2 MΩ cm^{-1} decarbonised water before being ashed in a furnace at 450 °C for 24 hours to avoid any contamination from residual organic carbon. The clean bottles were autoclaved before use.

2.3.2 Preparation of organic and inorganic nutrients

The inorganic nutrient mix was prepared by adding 100 mL of 4.67 mM NH_4Cl, 100 mL of 1.47 mM KH_2PO_4, 5 mL of non-chelated trace elements, and 5 mL of selenite-tungstate (SeW) solution in a 250 mL beaker on a magnetic stirrer at 300 rpm.

The non-chelated trace element solution was prepared according to Widdel et al. (1983). Deionised water (987 mL) was measured into a 1L ashed glass bottle on a hotplate magnetic stirrer at 300 rpm and 12.5 mL of 25% HCl (100 mM), $FeSO_4$. $7H_2O$ (7.5 mM), H_3BO_3 (0.5 mM), $MnCl_2.4H_2O$ (0.5 mM), $CoCl_2.6H_2O$ (0.8 mM), $NiCl_2.6H_2O$ (0.1 mM), $CuCl_2.2H_2O$ (0.01 mM), $ZnSO_4.7H_2O$ (0.5 mM) and $Na_2MoO_4.2H_2O$ (0.15 mM) were sequentially added. The trace element mixture was autoclaved in bottles tightly closed with rubber-fitted screw caps or fixed stoppers; a headspace of approximately 1/3 of the volume was left.

https://doi.org/10.5194/egusphere-2026-2864
Preprint. Discussion started: 4 June 2026

The SeW solution was prepared as reported by Widdel and Bak (1992). The NaOH (10 mM) was weighed into a 1 L bottle containing 1 L DH_2O on a hotplate magnetic stirrer stirring at 300 rpm, and added Na_2SeO_3. $5H_2O$ (0.02 mM) and Na_2WO_4. $2H_2O$ (0.02 mM) with constant stirring. The solution was then autoclaved.

The NH_4Cl (4.67 mM) and KH_2PO_4 (1.47 mM) were also prepared as reported by Widdel and Bak (1992). The solutions were autoclaved.

2.3.3 Filtration of surface water sample and concentration of microbes

The surface water was first filtered using a vacuum pump mounted with a 0.7 µm GF/F, 47 mm diameter to remove the particulate organic matter. Microbes were subsequently collected on the 0.2 µm nylon membrane (NM) filter by re-filtration of 0.7 µm GF/F filtrate. To ensure an approximately equal number of microbial cells were collected on each filter, an equal volume (100 mL of 0.7 µm GF/F filtrate) was used on each NM filter. The 0.2 µm NM filters were used as inoculum for the experiment.

2.3.4 Setting up the microcosm

The serum bottles were prepared and labelled as indicated in Fig 2 and Table 1:

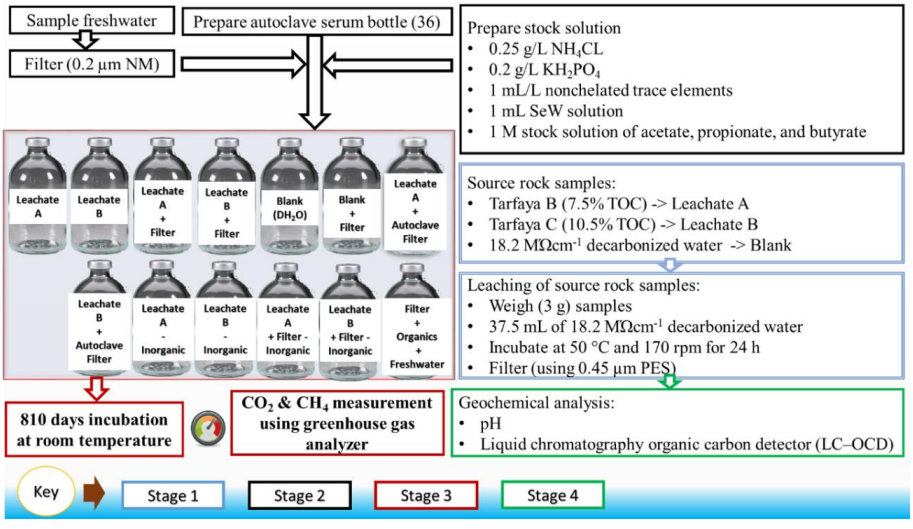

Figure 2: Schematic overview of the experimental setup (Modified from Horstmann (2018)).

The microcosm set-up consisted of bottles with testing materials (leachate A and B) as a source of C substrate, plus the inoculum filter and six control groups, as summarised in Table 1. Each microcosm setup was prepared in triplicate to measure variation in the experiment so that statistical tests could be applied to evaluate differences and assess reproducibility.

https://doi.org/10.5194/egusphere-2026-2864
Preprint. Discussion started: 4 June 2026

Filters (0.2 µm NM) were placed in all microcosm bottles except uninoculated controls. Autoclaved control bottles with wet filters were autoclaved before the addition of leachate. The 10 mL of the given leachate was added to all microcosms except the blank and positive controls. The 10 mL of the blank (18.2 MΩ cm^{-1} decarbonised water) was added only to blank controls. The 4 mL inorganic nutrients mix was added to all microcosms except A-inorg, B-inorg, A + F-inorg and B + F-inorg, in which instead 4 mL of 18.2 MΩ cm^{-1} decarbonised water was added to bring about the same volume as the other microcosms with an inorganic amendment. 28 µL each of acetate (2 mM), propionate (2 mM), butyrate (2 mM), and 10 mL filtered freshwater (filtered with a 0.45 µm PES filter) was added to the positive control. The rubber stopper was placed onto every serum bottle and sealed with an aluminium cap. The microcosms were stored in the box (away from sunlight to avoid photo mineralisation or degradation) at room temperature.

Table 1: Microcosms treatment groups, description, and rationale behind each control group

Treatment Group	Treatment (microcosm) ID	Description	Reasons
Inoculated sample	A+F and B+F	These contained testing materials (leachate A and B) as sources of C substrate, plus the inoculum filter.	To study whether the introduced microbes can biodegrade the DOM derived from the leachates.
Filter control	Blk+F	The set contained only decarbonized (18.2 $MΩcm^{-1}$) water and an inoculum filter.	To investigate the filter response due to incubation. To assess whether changes in A+F and B+F are associated with the leachates or the filter itself due to OM carryover from the freshwater sample. **Note**: We assumed the filter might not collect only microbes, but with particulate OM that may get mobilized in the decarbonised water and potentially utilised by the microbes.
Blank Control	Blk	Decarbonised (18.2 $MΩcm^{-1}$) water without any C amendment (i.e., without Tarfaya black shale-derived DOM, surface water-derived DOM or any added nutrients) or inoculation.	To observe any response from the decarbonised water.
Positive control	F+Org+FW	Contained freshwater-derived DOM and added organic substrates (acetate (2 mM), propionate (2 mM) and butyrate (2 mM) acid) instead of Tarfaya black shale-derived DOM as a C source to the microbes. **Note**: the freshwater was autoclaved before addition.	To provide the microcosm with excess organic and inorganic nutrients to observe whether the filter inoculum can produce CO_2 and CH_4.
Non-inoculated control	A and B	Abiotic controls: Contained leachate only (no inoculum filter).	To investigate whether the shale samples contain indigenous microbes which may be activated through the process or to monitor any abiotic changes of DOM throughout incubation.
Autoclaved control	A+aut.F and B+aut.F	The inoculum filters were autoclaved before the addition of leachate.	To assess whether changes in A+F and B+F are associated with the presence of the filter itself, rather than living microbes in the filter.
Inorganic nutrient control	A-inorg, B-inorg A+F-inorg, and B+F-inorg	The inorganic nutrients were not added to this group.	To assess whether shale-derived DOM (A+F and B+F) contain sufficient inorganic nutrients to sustain biodegradation.

Key; A and B =leachate A and B, F= filter, Blk = blank (18.2 MΩcm-1 decarbonized water), FW = freshwater, aut.F= autoclaved filter, inorg= inorganic amendments, org= organic amendments.

Changes in CO2 and CH4 concentrations in the microcosms' headspace were measured using a GHG analyser at 1, 5, 9, 23, 54, 97, 275, 580, and 810 days of incubation and recorded. For quality assurance, a new calibration was performed after each GHG analyser's maintenance service or longer measurement intervals. All calibration correlation coefficients (R^2) fall within the range of 0.9989 to 1.0000 at a 99.5 % confidence interval. The wider gaps in measurement days between 97, 275, 580, and 810 days were due to the laboratory's inaccessibility during the subsequent

https://doi.org/10.5194/egusphere-2026-2864
Preprint. Discussion started: 4 June 2026

COVID-19 lockdown. This might favour the anaerobic microbes to grow as there is no ventilation (no oxygen supply) of the headspace within the interval time. Upon termination of the experiment on day 810, the inoculum medium of microcosm A + F and B + F, and other filter and positive controls (Blk + F and F + Org + FW) in which we observed substantial microbial response (considerable generation of biogenic CO_2) were further analysed for biotransformation of DOM. The medium was split into two, 6 mL + ¼ filter fractions, which were stored at -80 °C for potential DNA extraction and qPCR, while ~7 mL of the remaining sample was filtered using a 0.45 µm PES filter and analysed using LC-OCD for potential biotransformation/degradation of DOM.

2.4 Analytical Procedures

Several analytical techniques were applied to characterise the % TOC and kerogen type of the black shale samples, and the leachate's DOM before and following incubations. The % TOC, thermal maturity, and kerogen type were analysed using elemental analyses and Rock-Eval pyrolysis performed on bulk sediments (data from Kolonic et al. 2005). LC-OCD was applied in this study to investigate the trajectory chemical changes of DOM in microcosms. A GHG analyser was used to measure the change in CO_2 and CH_4 in the microcosm headspace over time.

2.4.1 Liquid chromatography – organic carbon detector – organic nitrogen detector (LC-OCD-OND)

The LC-OCD-OND model 9 was used to measure the change in DOM quantity and compositional organic fractions change with incubation. All glass vials were ashed, and for reproducibility, each sample replicate was run twice on the SEC from which the mean value and relative per cent difference were determined. Initially, the aliquot of 400 µL filtered leachate was diluted with 7.6 mL 18.2 MΩ cm^{-1} decarbonized water (1:20 v/v) in an ashed glass vial (the dilution was to ensure the measured DOM concentration is within the instrument calibration range, 0.5 – 5000 µg/L), and prepared for LC–OCD analysis. After 810 days of incubation, the experiment was terminated. The serum bottle was de-crimped, a sterile syringe (60 mL) with PES 0.45 µm was rinsed with 18.2 MΩ cm^{-1} decarbonized water, and then 7 mL of the incubation sample was poured from the top after removing the syringe piston and then the piston was inserted back. The first 2 mL that passed the filter was discarded to avoid contamination if residual OM hang in the syringe piston. The samples were then filtered into the glass vial. As the post-incubation samples still contain a higher amount of DOM beyond the LC-OCD calibrated measuring range, the A+F, B+F and Blk+F were appropriately diluted (1:15 v/v %) and F+Org+FW by 1:20 v/v % with 18.2 MΩ cm^{-1} decarbonized water before analysing them in LC–OCD. ChromeCalc software was used to manually integrate sample peaks as presented in section 3.6.4 (Fig 3.4; Table 3.1)

https://doi.org/10.5194/egusphere-2026-2864
Preprint. Discussion started: 4 June 2026

2.4.2 GHG-GC analysis

The gas chromatograph with a flame ionisation detector (GC – FID) was used to measure the concentration of CO_2 (via a methanizer) and CH_4 in the headspace of the microcosm during the incubation period of 810 days. To measure the GHG from the headspace, the cap of the serum bottle was wiped with ethanol, and a volume of 5 - 10 mL was taken off the headspace using a 10 mL syringe mounted with a needle (Fig 3). The needle was flushed with 2 mL of the sample gas before being injected under constant pressure (19-21 ml/min equal to the injection pressure of calibration) into the GHG analyser. The headspace was ventilated with air (re-introduction of oxygen) on 54 and 275 days of incubation by injecting atmospheric air equivalent to the total volume of the samples taken out. The syringe filter (0.2 µm) was mounted on the syringe during the injection of atmospheric air into the microcosm. The change in the concentration of the CO_2 and CH_4 with re-ventilation was calculated using the derived equation 1.

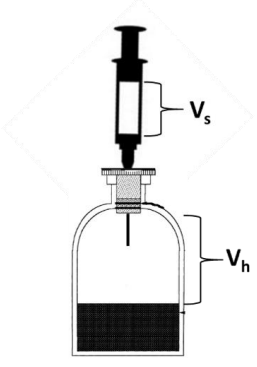

Figure 3: Diagram of the microcosm system

$$C = C_1 - \frac{V_s}{V_h}(C_1 - C_2) \qquad 1$$

Where C is the change in concentration of CO_2/CH_4 in the headspace, C_1 is an initial concentration of CO_2/CH_4 in the headspace, C_2 be a concentration of CO_2/CH_4 in air, V_h is the volume of the headspace and Vs be the volume of the amount taken in the syringe.

A requirement for the quantification of GHGs produced from the black shale leachate microcosm headspace required appropriate gas-phase calibration standards to determine absolute concentrations. Following the very high CO_2 production observed in the initial microcosm test phase the calibration was extended to up to 30% (300000 ppm).

https://doi.org/10.5194/egusphere-2026-2864
Preprint. Discussion started: 4 June 2026

3.0 Results

3.1 Molecular composition of DOM in the leachates

The LC-OCD results showed that black shale sample B (10.5 % TOC and of kerogen Type I) released more DOM (41.34 mg/g rock) than sample A (7.5 % TOC and kerogen Type I/IIs) which released 17.78 mg/g rock. Both samples contain 9 identifiable compound groups (Fig 4), which range from macromolecules (X1, X2, and X3; large groups of compounds with molecular weight >350 Da) to low molecular weight groups (X4 – X9; MW <350 Da). The DOM of the shale leachates was characterized by one prominent peak, X4, eluted at a retention time range of 23.35 – 30.82 minutes in the chromatogram, contributing 38.3 and 42.0 % in leachate A and B to the total DOC. This peak is considered to represent low molecular weight organic acids fraction (X4; Huber et al. (2011); Zhu et al. (2015)). OM mobilised from kerogen is generally believed as the source of LMWOAs and their generation is considered to result from an early stage of thermal maturation; Diagenesis (Zhu et al., 2015) or hydrolysis of cross-linked esters within the macromolecular network of kerogen (Siskin and Katritzky 1991). The concentrations of DOM acids extracted from the shales were validated against the initial kerogen oxygen content of the Tarfaya shale samples. The samples are thermally immature. The immature kerogen contains significant amounts of aliphatic components and oxygen ((Zhu et al., 2015; Leins et al. 2022). The oxidation of n-alkanes during geological times might also lead to the formation of LMWOAs. Thus, the higher relative proportion of X4 in B compared to leachate A (17.36 vs 6.81 mg/g rock) likely reflects an elevated release from the high pyrolytic kerogen S2 yields, expressed in the S2/S3 ratio (18.55 vs 13.77).

Table 2 indicates the different compound groups eluting at different time ranges and molecular sizes from the LC-OCD column. The LC-OCD results of the sample leachates (A and B) showed the first peak at 15.18 – 18.62 minutes retention time, representing macromolecule X_1 with the largest molecular size. The X1 fraction contributed 1.9 and 0.9 % to the total DOM. The peak X_2 observed at 18.62– 20.87 minutes contributed 5.9 and 8.9 % and had a lower MW than X_1. The peak eluted at 20.87 – 23.35 minutes represents macromolecule X_3 (MW < X_2), which contributed 19.7 and 12.7 % to the total DOM. We identified low molecular fractions (X_5 – X_9), which are composed of high molecular weight neutrals (X_5 and X_6), intermediate neutrals (X_7 and X_8), and very low molecular weight neutral (X_9) in both leachates. The two peaks X5 and X6, which cumulatively contributed 24.9 and 17.8 % in leachate A and B to the total DOM, had a residence time range of 30.82 – 40.07 minutes. The intermediary neutrals observed at 40.07 – 46.95 minutes contributed only 10.0 % and 4.8 % to the total DOM. The very labile fraction X_9 eluting at the tail end of the chromatogram at residence time range 46.95- 70 minutes, contributed 7.0 and 6.0% to the total DOM.

https://doi.org/10.5194/egusphere-2026-2864
Preprint. Discussion started: 4 June 2026

Table 2: Description of LC-OCD fractions; Modified from Huber et al. (2011), Penru et al. (2013), and Zhu et al. (2015).

This study fractions		Fraction (Huber et al., 2011)	Molecular mass range (Da)	Properties	Description
Macro-1	X1	Biopolymers	>10,000	Not/little UV-absorbable, hydrophilic	Polysaccharides and proteins
Macro-2	X2	Humic substances	>1000	Highly UV-absorbable, hydrophobic	Calibration based on Suwannee River standard from IHSS
Macro-3	X3	Building blocks	350 – 500	UV-absorbable	Break down products of humic substances
Acids	X4	Low molecular weight acids	<350	Negatively charged	Low molecular weight aliphatic acids
Neutrals	X5 – X9	Intermediate – low molecular weight neutrals	<350	Weakly or uncharged hydrophilic, amphiphilic	Alcohols, aldehydes, ketones, amino acids

The compound groups X1 – X4 (in black) are reported by Zhu et al. (2015), while X5 – X6 (in red) are additional peaks (compounds) reported in this work.

Both leachates have moderate UV absorbance with a relatively higher response from leachate B (UV absorbance: A = 11.67 AU, B = 24.48 AU), indicating the presence of aromatic/unsaturated compounds. Both leachates show similar concentrations of total dissolved nitrogen (A = 3.27 mg/g ON, B = 3.43 mg/g ON).

3.2 Changes in the molecular composition of DOM related to microbial activity

The LC-OCD was used to investigate the change in DOM compositions in the microcosms over 810 days of incubation (Fig 4). The results of pre-incubation leachates indicated that the relative contribution of lower molecular weight (LMW) compound groups (X_4 – X_9) to total DOM was ~ 80 % and 70 % for leachate A and B, respectively. However, after the incubation, the detected compound groups showed a marked decrease in the % contribution of LMW compounds to ~50 % and 52 % for inoculated leachates A and B microcosms, with LMWOA (X_4) decreasing by 23 % and 25.5 %. Also, the very labile carbon group (X_9) decreased from 6.5 % to 0.2 % and 5.9 % to 0.3 % in inoculated leachates A and B microcosms (Fig 4). The % relative contribution of the humic-like macromolecules (X_1, X_2, and X_3) stand as 7.2±0.7, 5.0±0.2 and 37.9±0.5 % in inoculated leachates A, and 4.2±1.0, 11.2± 3.2 and 35.5±1.9 % in inoculated leachates B microcosms, which are relatively higher than in pre-incubation leachates A and B (1.9, 5.6 and 12.7 % and 0.9, 8.9 and 19.7 %).

The filter control microcosm (Blk+F) displayed a % relative contribution of the humic-like macromolecules X_1 and X_3 (3.6 and 30.4 %), lower than the samples inoculated microcosms with X_2 (12.4 %) slightly higher.

https://doi.org/10.5194/egusphere-2026-2864
Preprint. Discussion started: 4 June 2026

The positive control (F+Org+FW) exhibited a similar macromolecular pattern to the filter control, showing lower X_1 and X_3 (1.7±0.14 and 17.1±0.4%) and prominently higher X_2 (46.7±1.0%) than the microcosm with leachates. The % relative contribution to the total of high molecular weight neutral group (X_5) increased after incubation in both leachates inoculated microcosms (23.2±2.8% and 21.0±3.0% for A+F and B+F) and filter control (35.3 %) compared to pre-incubation leachates (10.1 and 5.4% for A and B). Unlike the sample inoculated microcosms, where lower molecular fractions disappeared with the incubation, we observed a marked increase of X_8 (6.4±0.6 %) and a slight change of X_9 (3.2±0.1%) in the positive control.

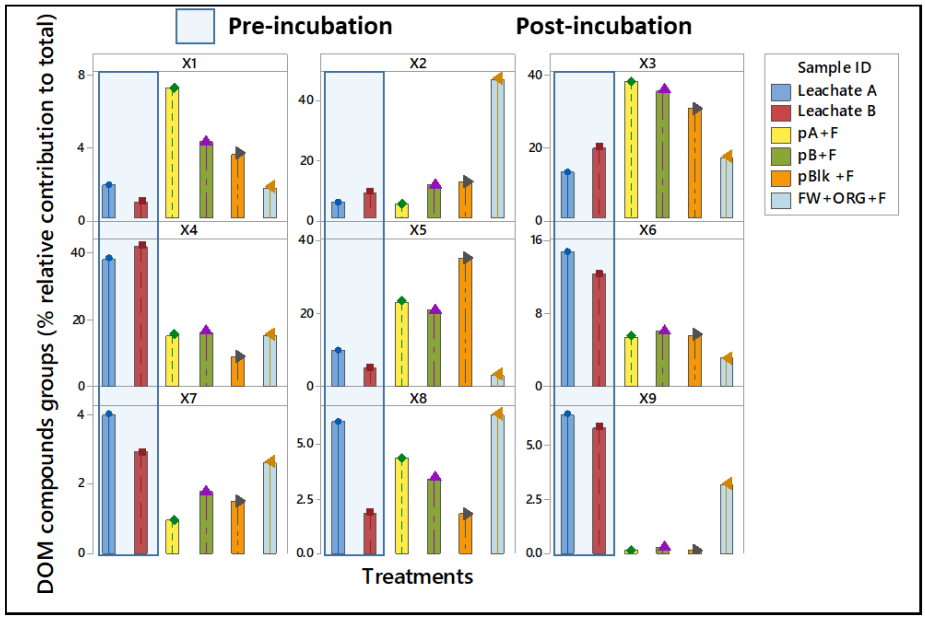

Figure 4: DOM composition of pre- and post-incubation samples (% relative contribution to total DOM) measured by LC-OCD. The relative proportion was the mean value of the triplicates. Key: P, post-incubation samples. A and B represent sample leachates, blank (Blk); deionised water, F; filter, FW; freshwater, aut.F; autoclave filter, Org; organic, and inorg; inorganic amendments (Table 4.1). X1, X2, and X3; large groups of compounds with molecular weight >350 Da), and low molecular weight groups (X4 – X9; MW <350 Da) (refer to Table 3). This data suggests the degradation of labile compounds (X4 -X9) with the formation/increase in macromolecules X1 – X3 and LMW X5.

Stoichiometric calculations were applied to determine how much organic carbon was degraded to produce the observed CO_2 and CH_4, and how much total organic C was lost from the leachates. The following assumptions were made: no external organic carbon source in addition to what was present in the leachates, and an inoculated filter (which carries over freshwater OM) in the sample inoculated microcosms. Therefore, the organic feedstock for the microbes should be either C from the leachates, inoculated filter or contributions of necromass (dead cells).

https://doi.org/10.5194/egusphere-2026-2864
Preprint. Discussion started: 4 June 2026

We already know the amount of dissolved C in our leachates; therefore, we need to determine the amount contributed by the necromass and filter.

For the necromass contributions, we need to know the actual amount of cells that we have in the microcosms and C cell^{-1}. Braun et al. (2016) quantified amino acids in Baltic Sea sediments and calculated cell-specific carbon content on the order of 19 to 31 fg C cell^{-1}. The abundance of cells in both oil sands and formation water has been previously estimated to be between 10^4 and 10^7 cells g^{-1}, with the highest cell densities found at the oil–water transition zone (Bennett et al., 2013). Although we don't have the quantitative data of the cells in our microcosms, we assumed the highest values obtained by Bennett et al. (2013). The reaction mixture in our microcosms was ~ 18 mL, therefore, the estimated number of the cells in our inoculated microcosms is 1.8 x 10^8 cells per microcosm. If we assumed 75 % of the cells were utilized by saprotrophs, then the amount of C necromass contributions can be estimated as 4.19 µg C.

For the filter control contributions, we need to know the actual amount of C carried over by the filter from freshwater. Since we observed the breakdown of the filter during incubation, we might suggest also that there was a degradation of the C substrate from the nylon inoculum filter. Therefore, to estimate the inoculum filter control contributions we need to determine the amount of carbon the inoculum filter released in the microcosms, whether it continuously released DOM with depletion of DOM due to microbial degradation in the microcosm and the amount of carbon that remained on the filter (undissolved) after the incubation. These might be very complex and difficult to analyse. However, in this research work, since all the inoculum filters underwent similar treatments, we assumed; the filter contributed a relatively similar amount of C in the inoculum leachates and filter microcosms. To eliminate the filter contributions, we subtract the filter microcosms from the sample microcosms. This approach has previously been used by Miles and Doucette, (2001).

DOM concentration of the leachates subsequently decreased after the incubation (A; 17.78 to 4.01 mg/g, B; 41.34 to 9.66 mg/g; Note; the post-incubation concentrations were calculated after filter correction; to get the residual DOM of leachates after the incubation period, the post-incubation concentrations in filter control (Blk + F) was subtracted from the inoculated samples (A+F and B+F). The results suggest mineralization of 13.77 and 31.68 mg/g DOM of leachate A and B.

Biodegradation does not only mineralize DOM but also bio-transform and generates other OM compounds as by-products, i.e., monomer carbohydrates, low molecular alcohols, polypeptides, to low-molecular-weight monomers, e.g., amino acids and urea (Antia et al., 1991; Zehr and Ward, 2002). Some of these by-products contain aromatic and unsaturated compounds. The total UV absorbance was used as a quantitative measure to infer aromatic/ unsaturated compounds formed or utilised in the DOM compound groups by microbial activity at the end of the incubation. The

https://doi.org/10.5194/egusphere-2026-2864
Preprint. Discussion started: 4 June 2026

composition of the pre-incubation leachates was generally lower (11.67 and 24.48 Absorption Unit {AU}) compared to post-incubation samples (Fig 5). The inoculated samples' microcosms exhibited 40.58±2.67 and 53.38±15.38 AU for A+F and B+F, while the positive control (F+Org+FW) showed relatively significant UV absorbance (544.84±1.10 AU; in which X_2 contributed to 75.4±0.8 % relative to total) and Blk+F, which had a 37.7 AU in which X_2 contributed 46.7 %, respectively. The relative UV absorbance increases in the macromolecule X_2 across the post-incubation microcosms with positive and filter controls revealed more significant absorbance. The % relative increase in the contribution of high molecular weight neutrals (X_5) by ~15% to the total DOC coincided with the increase in their UV absorbance in the sample inoculated microcosm (14.0±0.7% for A+F and 15.4±1.4% for B+F), and 10.2 % in filter control samples while showing no UV absorbance response in the pre-incubation leachates and positive control. The Lower molecular weight neutrals (LMWN; X_5 – X_9) in pre-incubated leachates showed elevated UV absorbance (34.1 and 33.3 % relative to the total absorbance) compared to the inoculated sample (B+F; 18.8±3.0 %), filter control (Blk ± F; 14.4 %), with the positive control (FW+Org+F; 2.3±0.4 %) showing the least absorbance.

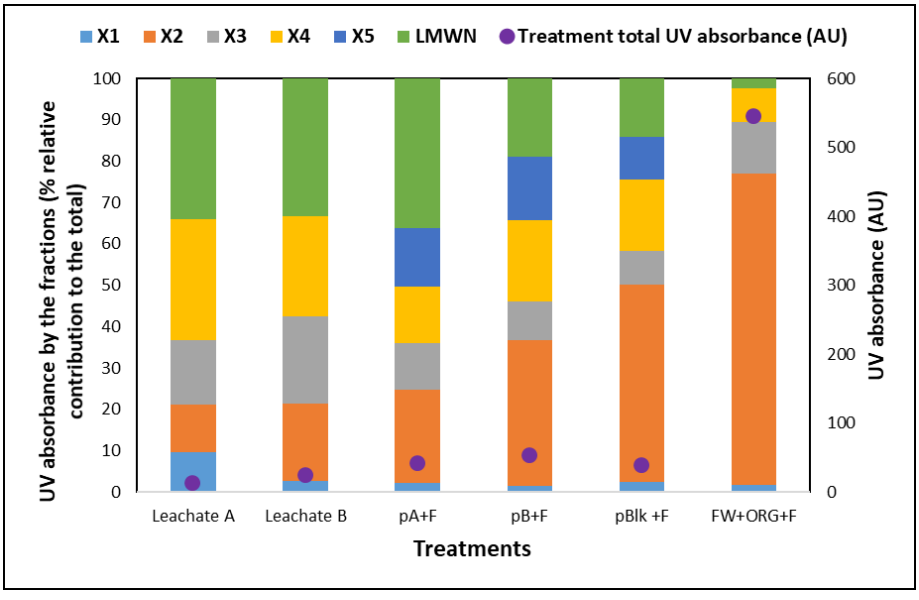

Figure 5: UV absorbance of samples and % relative contribution to the total by the detected compound groups. These reflect the formation of LMW condensed aromatic group X5 and biotransformation of DOM toward more recalcitrant and highly aromatized/unsaturated macromolecule group X2.

A higher C/N ratio of the samples before the incubation was observed (5.44 and 12.05 for leachate A and B, respectively) (Fig 6). The C/N was notably lower (compared to leachates) after the incubation in the inoculated leachates microcosm and controls (filter and positive control): 0.41, 0.43, 0.97 and 1.54 for A+F, B+F, Blk+F and F+Org+FW, respectively. This might suggest the

https://doi.org/10.5194/egusphere-2026-2864
Preprint. Discussion started: 4 June 2026

substantial mineralization of the DOC or there was a lot more DON in the surface water which was carried over by the filter in pA+F, pB+F, and pBlk+F.

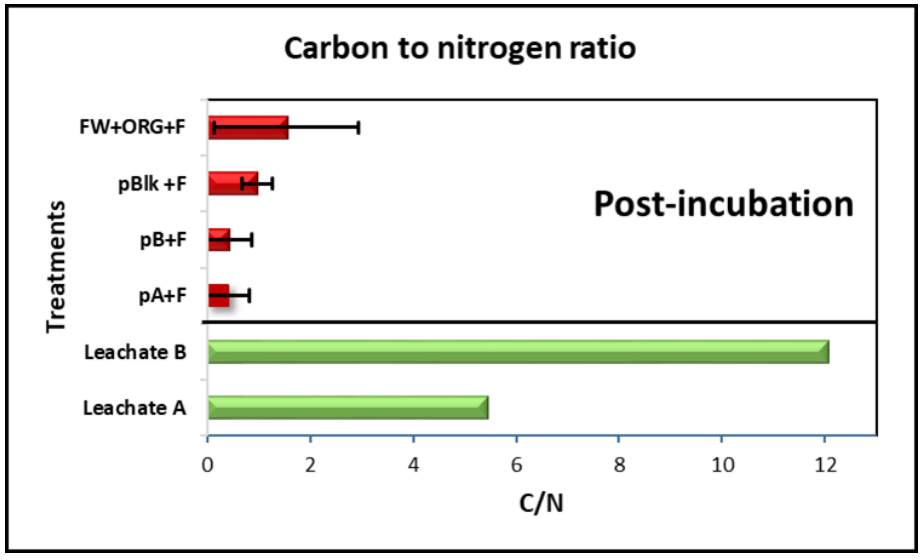

Figure 6:: Carbon to nitrogen ratio of pre and post-incubation samples indicating a drastic drop in C/N ratio, which signified mineralization of C substrate from the DOM pool. Note: The C/N was calculated by dividing the total DOC by the total DON.

3.3 Microbial Growth and GHG Production

3.3.1 Carbon dioxide - CO_2

The production of CO_2 and CH_4 in the headspace of the triplicate microcosms was monitored for 810 days with recurrent measurements of the headspace of CO_2 and CH_4 using a GHG-GC analyser. The cumulative mean CO_2 and CH_4 concentration over time (days) and calculated standard errors from the triplicate measurements from microcosm headspace samples are presented in Figs 7 and 8 and fully reported in Appendix I and II. Fig 7A showed that the inoculated sample microcosms headspace means CO_2 concentrations of 1307±4 and 1195±7 ppm for A±F and B±F on the first day of incubation which was twice the measured laboratory atmospheric concentration (445 ppm) and the blank control. The mean CO_2 concentration doubled after 23 days of incubation and reached 7596±917 ppm for A+F and 8002±449 ppm for B+F at 97 days. Substantial production of CO_2 was observed at 580 days of incubation, raising the headspace CO_2 concentration to 107113±4414 ppm and 113585±443 ppm for A+F and B+F. The cumulative mean concentrations reached a peak at 810 days, totalling 120779±1720 and 125278±1462 ppm for A+F and B+F microcosms (Fig 7A). These peak concentrations are 92 and 104 times the initial concentration (concentration on the first day) of inoculated sample

https://doi.org/10.5194/egusphere-2026-2864
Preprint. Discussion started: 4 June 2026

459 microcosms and 271 times the laboratory atmospheric air CO_2 concentration and blank control
460 (blk).

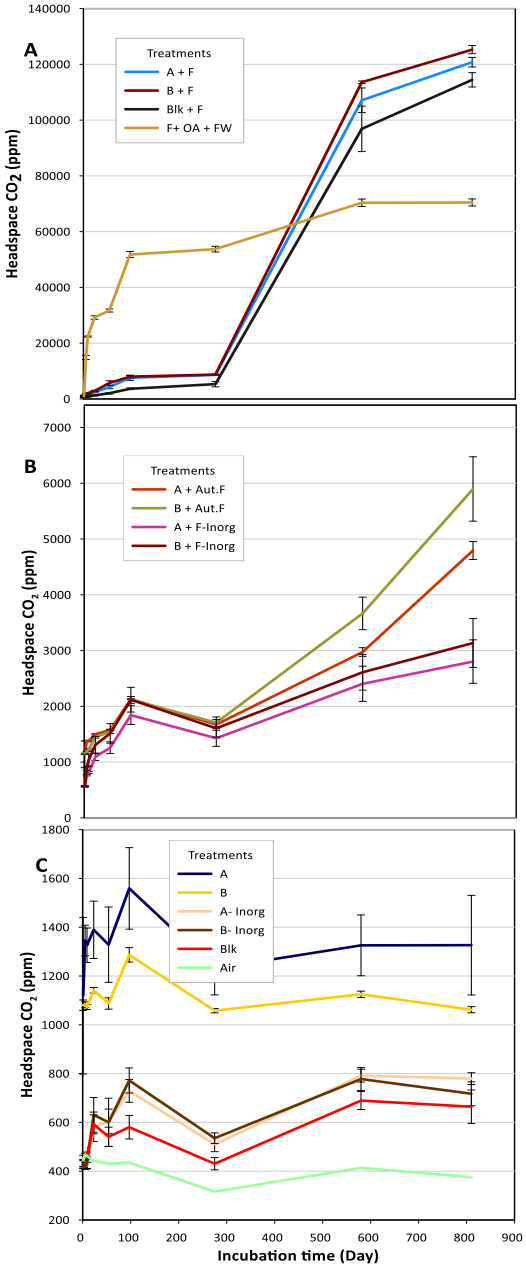

461

462 Figure 7: Measured headspace CO_2 mean concentrations of the different microcosms set up over time. Key;
463 A; Samples inoculated microcosm, blank, filter, air and positive controls. B; Autoclaved and inorganic
464 nutrients control. C; Uninoculated control group.

https://doi.org/10.5194/egusphere-2026-2864
Preprint. Discussion started: 4 June 2026

In the experimental control groups, the first control group (positive control; F + OA + FW) displayed a mean concentration of 1015±8 ppm CO_2 on the first day of the incubation (Fig 7A and appendix I). A rapid increase in CO_2 concentration was observed in the headspace of the microcosm after 5 days producing 14887±75 ppm CO_2 (which is 33 times high than blank control (blk) and measured atmospheric CO_2 concentration which serves as the reference point). The production of CO_2 continued rapidly until 23 days of the incubation reaching 29193±602 ppm CO_2, then slowed down. The F + OA + FW show the cumulative mean amount of CO_2 reached 70462±1270 ppm CO_2 after 810 days of incubation.

In Fig 7C, the blank (Blk) control showed a relatively similar CO_2 means concentration on the first day (472±16 ppm CO_2) with laboratory atmospheric concentration. The CO_2 concentration remains slightly the same throughout the incubation (810 days) with a cumulative mean concentration of 664±69 ppm CO_2.

The filter control (Blk+F) microcosms displayed similar headspace CO_2 concentrations as laboratory atmospheric air (472±16 ppm) on the 1st day of the incubation. However, the CO_2 concentration in the microcosm gradually continued to rise and reached 5317±969 ppm at 275 days of incubation. The massive CO_2 production was observed at 580 days (96860±8155 ppm) and cumulatively reached a peak at 810 days of incubation, totalling 114441±2565 ppm (Fig 7A).

The uninoculated control group (A, B, A-inorg, B-inorg) generally showed no significant change in CO_2 concentration in the headspace (from day 1 to 810), and headspace total concentration stands below 1600 ppm CO_2 at 810 days of the incubation (Fig 7C). In the Fig 7B, the autoclaved control (A+aut. F and B+aut. F) revealed a cumulative measured CO_2 mean concentration of 4795±162 and 5897±577 ppm for A+aut. F and B+aut. F in their headspace after 810 days of incubation. Also, the inorganic nutrients control group (containing leachates and microbes but without inorganic amendments; A+F – inorg, and B+F – inorg) cumulatively generated only ~3000 ppm CO_2 after 810 days of incubation.

3.3.2 Methane - CH_4

The CH_4 mean concentrations of the inoculated sample microcosms and controls are presented in Fig 8 and Appendix II. Data in Fig 8A showed that the mean concentration of CH_4 in leachate's inoculated microcosms remains relatively similar to laboratory air (3579 ppb) in the first 5 days of the incubation and slightly increases to 6132±216 and 5830±135 ppb for A+F and B+F, which were twice the atmospheric and blank controls after 23 days of incubation. The cumulative mean methane concentrations lowered to 5298±439 and 5148±1056 ppb (for A+F and B+F) on 54 days of incubation. And slightly increase to 5661±227 and 7775±1966 ppb (2 to 3 times atmospheric concentration) after 810 incubation days.

https://doi.org/10.5194/egusphere-2026-2864
Preprint. Discussion started: 4 June 2026

499 The low headspace CH_4 concentration was observed (relatively similar to atmospheric
500 concentration) throughout incubation time for the positive control (FW+Org+F) except at 9 and
501 54 days of incubation, which reached 5642±126 and 5857±56 ppb CH_4, respectively, and returned
502 to 4031±26 ppb at 810 days of incubation.

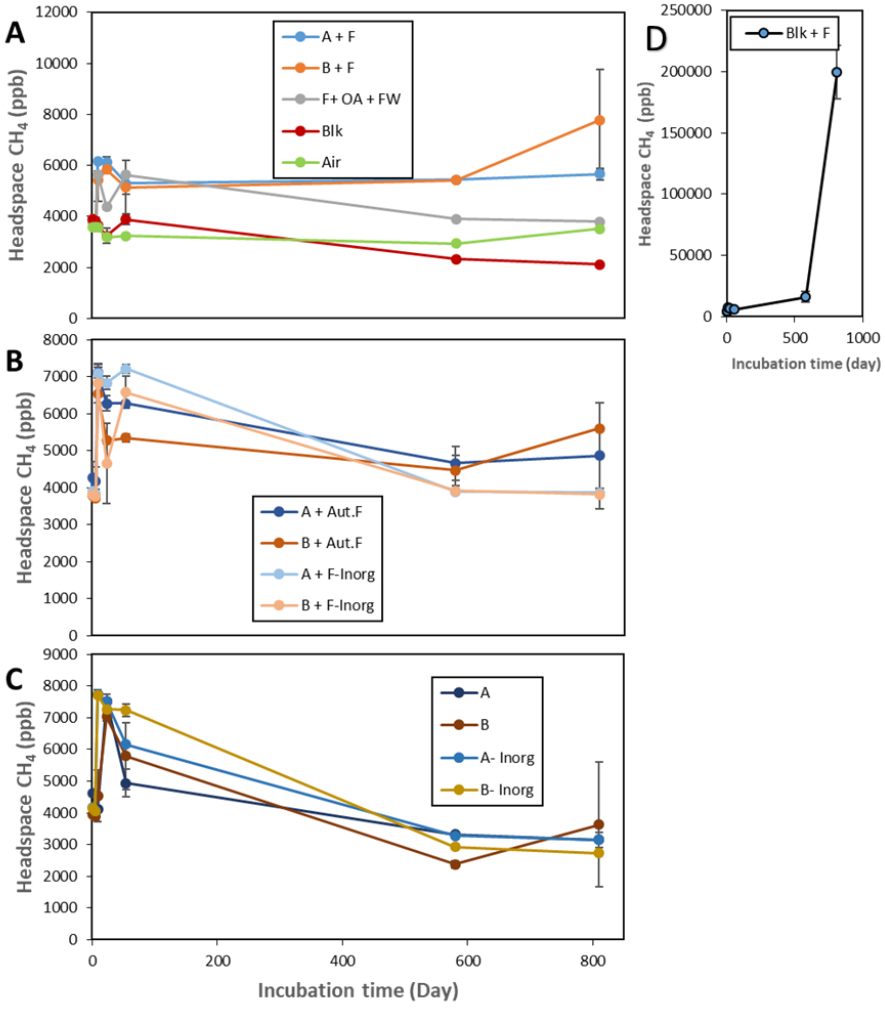

503

504 Figure 8: Measured headspace CH_4 mean concentrations of the different microcosms set up over time. Key;
505 A; Samples inoculated microcosm, and blank, air and positive controls. B; Autoclaved and inorganic
506 nutrients control. C; Abiotic control group.

507 The autoclaved, abiotic, and inorganic nutrients controls showed slightly similar headspace
508 methane concentrations (between 4167 – 3755 ppb) as the inoculated samples' microcosms in the
509 first five days of the incubations (Fig 8B and 8C). The abiotic controls showed no change in

https://doi.org/10.5194/egusphere-2026-2864
Preprint. Discussion started: 4 June 2026

methane concentration on the 9th day of the incubation and returned to atmospheric concentration after 810 days of the incubation time (Fig 8B).

The autoclave and inorganic controls showed an increase in headspace methane concentration (6545 – 7754 ppb) at 9 days of the incubation and remained slightly similar after 54 days of the incubation. The mean concentration drastically reduced to 3831±881 ppb in A+aut.F, while it rose to 9057±506 ppb in B+aut.F at 810 days of the incubation.

Both the filter and blank controls displayed the same mean CH_4 concentration measured in the headspaces of their microcosm with atmospheric conditions in the first and 5 days of incubation. The mean concentration of CH_4 in the filter control rises to 7146±1855 ppb on the 9 days and significantly upsurges to 16211±4417 ppb on 580 days and reaches a peak at 810 days, reaching 199413±21971 ppb CH_4 (Fig 8D).

4.0 Discussion

Despite the importance of DOM-microbial interactions in the natural and perturbed environment, little is known about the interaction and availability of rock-derived DOM to subsurface microbes, microbe-stimulated DOM transformations/degradation, and the resultant biogenic GHG formation in subsurface environments. In this study, we investigate the potential of immature marine black shale to stimulate microbial degradation and generate GHG (CO_2 and CH_4), and we applied analytical biogeochemical tools (LC-OCD) to document these changes in DOM chemistry and quantify the biogenic CO_2 and CH_4 generated from microbial activity.

For the set of biodegradation experiments, the GHG (CO_2 and CH_4) production in inoculated samples microcosms was compared with six control groups (these are: positive, filter, blank, autoclaved, abiotic and inorganic nutrients controls). The results from identically treated triplicate microcosms show good precision and reproducibility (RSD <15 %).

In the positive control microcosm (F+OA+FW), the microbes were introduced to their indigenous freshwater system with additional organic and inorganic nutrients. The massive production of CO_2 observed at the earliest stage of the incubation demonstrates that the microbial community collected in the freshwater was active and readily adapted to the microcosm system, which simulated their indigenous environment (freshwater). The rapid production of CO_2 may be related to the rapid utilisation of C substrate supplied to microbes to support their fast growth in the microcosm. Although there is no pre-incubation data for this microcosm, the biodegradation presumably generated highly aromatised humic-like macromolecule X_2 as dominant DOM fractions as observed in the LC-OCD data post-incubation (Figs 5 and 6) and generated very labile carbon (X_8 and X_9) as degradation products. These results are consistent with Wu et al. 2018 who incubated sediment-derived dissolved organic matter (DOM) and groundwater microbes and

https://doi.org/10.5194/egusphere-2026-2864
Preprint. Discussion started: 4 June 2026

continually analysed the microbial transformation of DOM over a 50-day incubation. Their results displayed a domination of less labile biopolymers (lipids) and lignin-like compounds at the end of the incubation. The decline in the production of CO_2 observed towards the end of the incubation might be related to either a limiting factor (electron acceptor or electron donor) or any physicochemical condition. It might also probably be due to a shift in the microbial community (natural selection) stimulated by the domination of highly aromatized humic-like macromolecule X_2, or a symbiotic relationship in which the microbially produced CO_2 was continually complexed to form the observed LMW organic compounds (X_8 and X_9) by CO_2 fixing microbes, possibly from a bacterial domain which survive a wide range of aerobic and anaerobic habitats (Saini et al., 2011; Wani et al. 2020).

In the earliest stage of the incubation (day 1), all the microcosms containing the leachates and inorganic nutrients (sample inoculated group; A+F and B+F, uninoculated control; A and B, and autoclaved control; A+aut.F and B+aut.F) showed similar headspace CO_2 concentration slightly above 1000 ppm (which is twice as high as atmospheric and blank control concentrations). This likely suggested that the recorded headspace CO_2 concentration might be due to the background respiration of the leachate samples, supported by the addition of inorganic nutrients. Similar results were reported by Horstmann (2018).

Unlike in the positive control, where we observed a short lag phase/ acclimation period (within the first 5 days), the leachate-containing inoculated microcosms (A+F and B+F) exhibited longer lag phases. In addition, we observed a slow production of CO_2 for around 3 months (97 days) of the incubation, generating ~8000 ppm. Since the abiotic controls headspace CO_2 concentration remained largely unchanged, suggesting the CO_2 generated in the inoculated samples microcosm's headspace was largely due to microbial activities. The slight production of CO_2 observed in the autoclaved controls throughout incubation may suggest that the autoclaving did not completely kill the microbes, and this was consistent with observations from Horstmann (2018). The slight increase in CO_2 concentration in the sample-inoculated treatments without inorganic nutrients (A+F-inorg and B+F-inorg) showed the significance of inorganic nutrients to microbial activities, as electron acceptors and donors must be present in large enough quantities (Nixon et al., 2012; Moore et al., 2025). A similar pattern with much lower headspace CO_2 concentrations was observed in the filter control (Blk+F) compared to sample-inoculated microcosms. The similarity in observed patterns might be because the filter supplied a large proportion of DOM (which is of freshwater origin to both microcosms). While the lower concentration might be due to poor carbon substrate availability (as 18.2 MΩ cm^{-1} decarbonised water was used in place of the leachate) and pH difference. Unlike the filter control, which contained only freshwater DOM, the inoculated samples' microcosms contained DOM of marine origin in addition to freshwater DOM. The aged source-rocks-derived DOM may be more

https://doi.org/10.5194/egusphere-2026-2864
Preprint. Discussion started: 4 June 2026

biologically available when mobilised through rock-water interactions, despite its lower concentration compared to the larger and possibly more stable freshwater DOM in the microcosm (Findlay and Parr, 2017). The DOM compound group compositions in marine black shale are highly dominated by LMWOAs and aliphatic LMWNs, while the surface water is majorly reported as dominated by macromolecular compounds (X1, X2, and X3) (Wilke et al. 2015; Yates et al. 2019; Aukes, et al. 2021). The LMWOAs and LMWNs are easily biodegraded by microbes compared to larger molecules (Wu et al. 2018). This might probably be the reason for the higher CO_2 concentrations observed in the inoculated sample microcosms at an early stage of the incubation compared to the filter control, confirming the immediate biodegradation of the leachate's source DOM.

The period of the lag phase may vary based on the environments that the microbes came from, as well as the condition of the microbes' cells themselves. If the growing cells are shifted from one type of media into the same type of media, which has similar environmental conditions, they will have the shortest lag period, as we observed in the positive control. Therefore, the slow production in the sample inoculated group may be related to the unusual environment and the C substrate introduced to the microbes. The leachates were derived from Cretaceous marine black shale, while the microbes were collected from the surface water. Therefore, the leachates from aged marine shale substrates might be unsuitable for immediate surface water microbes to grow; hence, they needed to adapt to the new environment (Wani et al., 2022). The microbial adaptation in different environmental conditions is mediated by complex cellular changes that keep physiology and metabolism, thereby ensuring survival (Wani et al., 2022). Adaptation may involve processes such as microbial growth, enzyme induction, or the exchange of genetic or molecular information to give the microbes substrate-degrading capabilities (Miles and Doucette, 2001; Wani et al., 2022). Therefore, an adaptation of the microbes to the new system might be the reason for the slow production. We also speculate that the carbon substrate from the leachates and shift in pH (filtered freshwater pH =8.34±0.10 and leachates pH = 7.51±0.10) might have stimulated a natural selection, in which the new conditions disfavour the dominant community and favour the rare biosphere, which leads to slow production.

The production of CO_2 continues to increase throughout the incubation (Fig 7) with a large production peak at 580 days of incubation, indicating that the microbes had already entered the exponential phase, with the development and rapid growth of a new adaptive microbial population, which concurrently increases microbial activity. A slowdown from the increase in production of CO_2 was observed after 580 to 810 days of incubation. This could indicate a change in microbial physiological state from activity and growth to maintenance, following depletion of labile C and LMWOA (X_6, X_7, X_9, and X_4) in the culture (Figs 4, 9, and 11).

https://doi.org/10.5194/egusphere-2026-2864
Preprint. Discussion started: 4 June 2026

Furthermore, the key cause for this decline might include a reduction in quantity and quality of inorganic nutrients or competition between microbes for depleted degradable C resources (X_9 and X_4) and with the dominance of the DOM pool by highly aromatised recalcitrant C (X_3 and X_2) as indicated by SEC data (Fig 4 and 11). Also, the shift in the DOM composition might lead to a microbial community shift (Wu et al., 2018). We have no direct evidence to discuss this community shift, but it could be that the populations that were growing on substrates are now exhausted and stopped growing, or growing more slowly, while others growing on less labile substrates have been and continue steadily growing the whole time, but more slowly than others. In a similar observation, Wu et al. (2018) described that the microbial composition was closely related to DOM turnover: microbial community in the initial stages of the incubation was influenced by relatively labile tannins (i.e., organic acids) and protein-like compounds, while in the later stage, the community composition evolved correlated with less labile lipids and lignin like compounds.

https://doi.org/10.5194/egusphere-2026-2864
Preprint. Discussion started: 4 June 2026

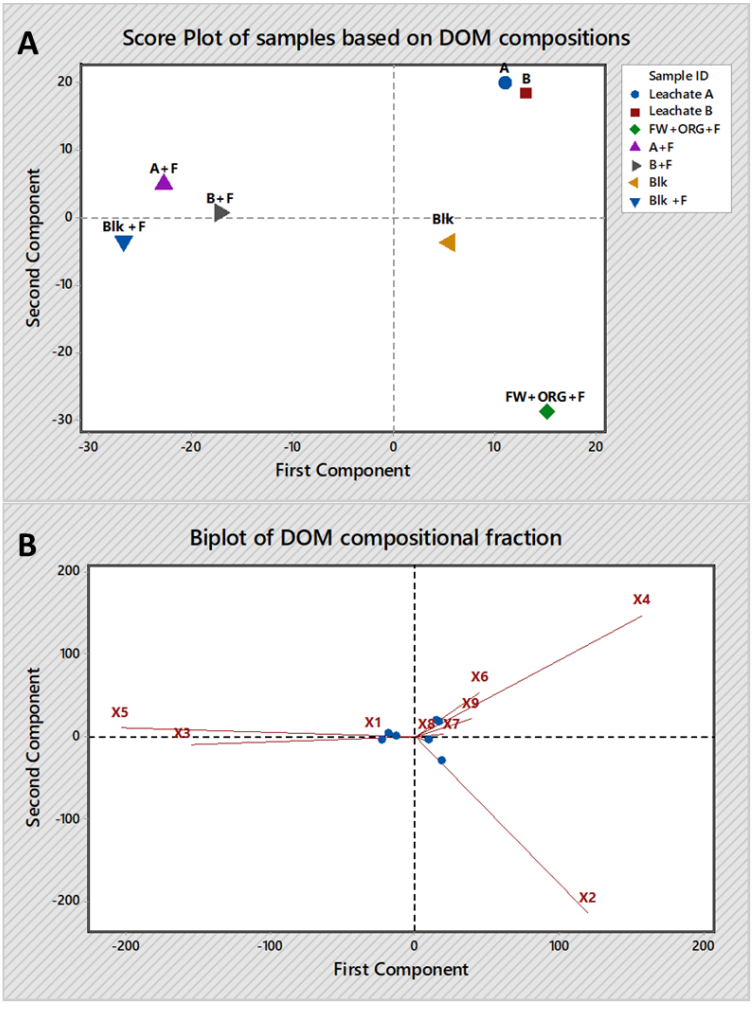

Figure 9: Eigenanalysis of the Correlation Matrix (ECM) score plot shows the correlation (90 %) of the samples based on their DOM compositions. The ECM analysis relates relatively similar samples based on their compositions. The analysis (panel A) reflected that the post-incubation inoculated sample groups (A+F and B+F) are slightly different from the filter control (Blk+F). Both are significantly different from the positive control. This suggests comparable (between the sample inoculated group and filter control) and different (with the positive control) metabolic by-products in the respective microcosms. The first component in the biplot (panel B) represents pre-incubation compounds in the leachates, showing the dominance of LMW groups (with X4 contributing the largest portion) with very low amounts of macromolecule groups (X1and X3) and LMW X5. It also displayed post-incubation compounds to the positive control, showing the dominance of lignin-like macromolecule X2. The post-incubation to the sample inoculated group in panel B displayed the dominance of macromolecule groups (X1 and X3) and LMW X5 with incubation. Note: the blue dots in panel B represent groups of samples as indicated in panel A.

Highly aromatized molecular weight neutrals were observed to be dominating the DOM pool as the experiment progressed to termination in the inoculated sample, filter control and positive control microcosms. The macromolecules X_1, X_3, and highly aromatised X_2 appear to be

https://doi.org/10.5194/egusphere-2026-2864
Preprint. Discussion started: 4 June 2026

recalcitrant to biodegradation, with X_3 continuously dominating the compound groups while X_2 dominated compound groups in the positive control (Figs 4, 9 and 11). The observed difference in response of the DOM pool to microbial activity in the sample inoculated microcosm and positive control may be related to the difference in the DOM source (DOM in the positive control is mainly terrestrial, while the DOM in the leachates is marine) and composition. The freshwater DOM composition is generally dominated by macromolecular humic fractions (Aukes et al., 2021), while marine DOM is dominated by LMW fractions (Kye et al., 2021). This suggests the potential for different metabolic pathways, as DOM type modifies the microbial population and their metabolic activities (Wani et al., 2022). The dominance of a recalcitrant C pool (X_2) with admixture LMW compounds (X_8 and X_9) in the positive control and the X_3 in the inoculated sample group, with the addition of microbial-derived recalcitrant (condensed aromatics X_5) compounds, suggest different metabolic pathways followed by microbial communities in these different microcosms.

The dominance of highly aromatic humic-like macromolecule group X_2 in the filter control microcosm reflects comparable patterns to the positive control (Fig 4), confirming a related freshwater DOM origin. The filter might have contributed the same freshwater DOM to the inoculated samples' microcosm. Based on the degradation of the inoculum filters we observed in the sample's inoculum and filter microcosms, the nylon filter not only carried over the freshwater OM but also supplied C itself. Based on our assumptions, there were three potential sources of C in the microcosms: the inoculum filter, necromass and leachates. The necromass C contribution was calculated/estimated as 4.19 µg. This amount is inconsequential compared to the large amount of CO_2 generated in the leachate microcosms.

For the filter contributions, it is difficult to estimate the amount of carbon inoculum filter released in the microcosms and whether it continuously releases DOM with depletion of DOM due to microbial degradation in the microcosm. Furthermore, we need to know the amount of carbon remaining on the filter (Undissolved) after the incubation. In this research, since all the inoculum filters underwent similar treatment in the sample's inoculum and filter control microcosm, we assumed that the filter may contribute a relatively similar amount of C to all inoculated microcosms.

To remove the filter contributions, we subtract the filter microcosms from the sample microcosms. The quantity of CO_2 measured in the filter control headspace microcosm was subtracted from the inoculated samples' microcosm. The calculated results are presented in Fig 10, reflecting maximum concentrations of CO_2 of ~ 11000 and 17000 ppm from the degradation of DOM in leachate A and B, respectively. Fig 11 showed filter-corrected DOM fractional compositions, derived from subtracting compound groups' contribution of the filter control from the inoculated

https://doi.org/10.5194/egusphere-2026-2864
Preprint. Discussion started: 4 June 2026

leachate microcosms. It exhibited clear utilisation across the DOM groups of the leachates during the entire incubation, indicating the transformation and utilisation of the DOM toward less biodegradable fractions (X_3 and X_1). Also, the X_4 might be the remnant that was yet to be degraded, and X_8 might be biodegradation remnants or by-products (Wu et al, 2018). The negative value of the compound groups X_2 and X_5 observed from the post-incubation filter corrected results (Fig 10), might be DOM groups that solely come from the freshwater DOM collected on the surface of the inoculum filter.

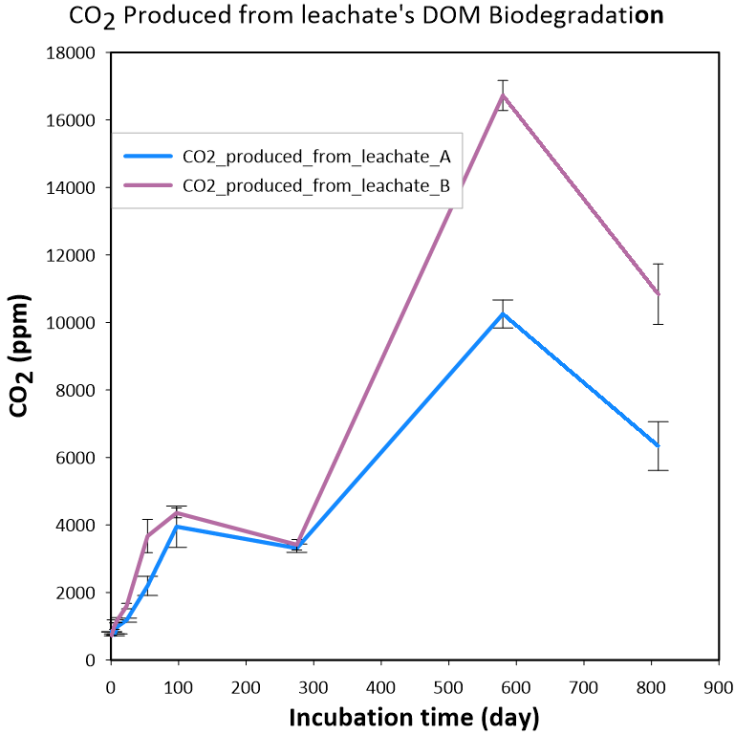

Figure 10: The amount of CO_2 produced from the leachate's degradation over time (filter control corrected).

https://doi.org/10.5194/egusphere-2026-2864
Preprint. Discussion started: 4 June 2026

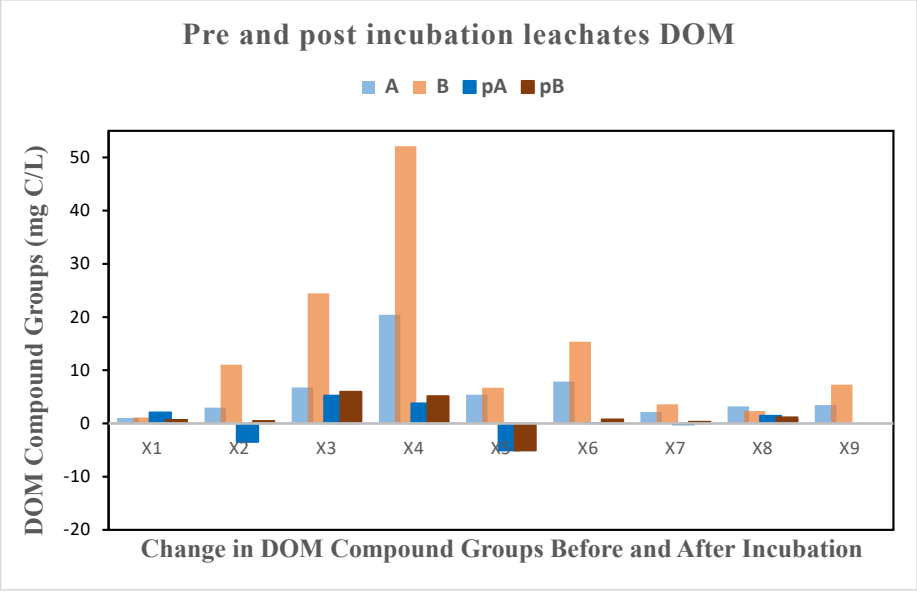

Figure 11: Post-incubation DOM fractional compositions (filter corrected). Key: pA = (A+F – Blk+F) and pB = (B+F – Blk+F). Note: The data were derived from subtracting the compounds group's contribution from the filter control from the inoculated leachate microcosms.

Nitrogen (N) is an integral component of DOM (Wiegnerand Seitzinger, 2004). Dissolved organic nitrogen (DON) is encompassed a continuum of compounds ranging from macromolecules (high molecular weight molecules), e.g., polypeptides, to low-molecular-weight monomers, e.g., amino acids and urea (Antia et al., 1991; Zehr and Ward, 2002), and hence can provide both C and N for microbial communities (Antia et al., 1991; Zehr and Ward, 2002; Berman and Bronk, 2003; Ghosh and Leff, 2013). In this study, the relative proportion of DON macromolecule compounds decreased gradually during incubation (Fig. 6), indicating that these DON compounds were likely continuously utilised by microorganisms when labile C was limited/ or simultaneously utilised, serving as supplementary C and N sources. The drastic decreases in the C/N ratio to incubation time across the microcosms indicate the mineralisation and biotransformation of the DOM pool (by removing carbon in the form of CO_2 from the DOM molecules, thereby decreasing carbon contents).

Low methanogenic activity observed in the sample inoculated microcosm with relatively similar headspace CH_4 concentration compared to the uninoculated control, suggested abiotic CH_4 production, presumably through low-temperature serpentinization and Fischer-Tropsch Type reactions (Duc, 2010; Okland et al., 2014; Moore et al., 2025). These low-temperature methanation reactions are described as likely to occur even at low pressure for wide geological settings (Etiope and Lollar, 2013). The higher CH_4 produced by the Blk+F microcosm than the leachate inoculum microcosm may be due to methanogenic activity. However, the produced

https://doi.org/10.5194/egusphere-2026-2864
Preprint. Discussion started: 4 June 2026

methane observed in the inoculated samples microcosm may not directly be linked to the biodegradation of the leachates, because of the pronounced methane produced by the inoculated filter control.

The important limitation of this microcosm experimental approach used in this research is that it is associated with an inorganic carbon sink. The headspace measurement does not account for the dissolved inorganic carbon (a certain amount of produced CO_2 might get dissolved/reacted in the reaction mixture in the microcosm). And the activities due to lithotrophs and methanotrophs may sink a certain amount of produced CO_2 and CH_4, which the microcosm's headspace measurement cannot account for.

Generally, in this experiment, it is observed that the DOM derived from Cretaceous marine black shale contributed to stimulating bioactivity and generating biogenic GHGs. The degradation of the DOM from the leachates generated approximately 11000 and 17000 ppm of CO_2 from the degradation of 13.77 and 31.68 mg/g DOM of leachate A and B (Fig 11). The higher CO_2 concentration generated in leachate B may be linked to the amount of DOM mineralised. The biodegradation also transformed the DOM toward less biodegradable fractions (X_3 and X_1). The observed X_4 might be the remnant that was yet to be degraded, and X_8 might be biodegradation leftovers or by-products from the microbial metabolic process.

4.1 Microbial Interactions with DOM in Geothermal Reservoirs: Implications for UKGEOS Mine Water Systems

Building on these results, drilling of the subsurface may likely lead to the generation of biogenic GHG from the biodegradation of mobilised aged rock-derived DOM. The microbes introduced to the subsurface during drilling, upon meeting favourable conditions in the borehole, can return to their full metabolic activity. An uncontrolled growth of the microbial community might lead to corrosion of the casing and formation of scales due to their metabolic by-products, changing the fluid chemistry in the perturbed subsurface reservoir (Inagaki et al. 2003; Westphal et al. 2019). The formation of highly recalcitrant macromolecules (X_1) and other remnant products (X_3, X_4, and X_8) might be a good example of the biodegradation products that may contribute to the alteration of the subsurface fluid chemistry and pose a threat to the plants. Biofilm formation from microbial growth can affect the flow rates and injectivity, due to the clogging of pores and filters (Brehme et al. 2020; Ábel et al. 2021), and even heat exchangers might lose their capacity as biofilms within the heat exchanger create an insulating effect at the surfaces where they are formed (Sand 2003). Hence, studying the DOM-microbial interaction in establishing and operating geothermal plants is critical.

The DOM type and source in the UKGEOS geothermal mine water site are strikingly complex and heterogeneous. However, this experiment generated insight into how both the terrestrial and

https://doi.org/10.5194/egusphere-2026-2864
Preprint. Discussion started: 4 June 2026

aged rock-derived DOM were transformed and mineralised in microbial activities. Hence, applying this approach to the UKGEOS samples might give more detailed information, which may be needed in the safe exploitation of this unconventional energy source.

5.0 Conclusions

The findings of this research have demonstrated that marine black shale-derived DOM stimulates microbial degradation that generates GHG, and the microbial activities bio-transformed and changed the property and molecular composition of DOM. SEC analyses of water-leached DOM from original shale and post-microcosm experiments identify the DOM groups of both sets of samples that are accessible to immediate microbial activity and recalcitrant C groups and document trajectory changes in DOM composition. Turnover and mineralisation of DOM have been observed, suggesting degradation of LMWOA and labile C by surface microorganisms. The data suggest that microbial metabolic activity affected the transformation of individual DOM groups (macromolecules X_1, X_2 and X_3, and LMWOA X_4), while producing compounds that contribute to the X_5 DOM fraction, resulting in dynamic changes in DOM property and composition induced by microbial interaction. Our results demonstrated that C cycling in an environment was orchestrated by a microbial activity that utilised specific C pools in available DOM. In engineered perturbed environments, such interactions between DOM and microorganisms dictate the ultimate fate of C.

6.0 Appendices

Appendix A: Mean CO_2 concentration and standard error of the triplicate measured in each microcosm headspace.

	Day(s)																	
	1		5		9		23		54		97		275		580		810	
Sample ID	$\bar{x}CO_2 \pm SE$(ppm)		$\bar{x}CO_2 \pm SE$(ppm)		$\bar{x}CO_2 \pm SE$(ppm)		$\bar{x}CO_2 \pm SE$(ppm)		$\bar{x}CO_2 \pm SE$(ppm)		$\bar{x}CO_2 \pm SE$(ppm)		$\bar{x}CO_2 \pm SE$(ppm)		$\bar{x}CO_2 \pm SE$(ppm)		$\bar{x}CO_2 \pm SE$(ppm)	
Air	445	-	468	-	462	-	443	-	430	-	436	-	316	-	414	-	375	-
A	1119	321	1345	63	1326	70	1389	117	1328	154	1559	167	1231	108	1326	125	1326	204
B	1080	21	1082	12	1073	10	1142	11	1087	23	1287	29	1058	9	1125	13	1062	12
A + Aut.F	1139	240	1380	6	1377	14	1499	10	1577	14	2126	10	1674	35	2974	77	4795	162
B + Aut.F	1147	12	1192	7	1219	19	1447	16	1545	32	2115	60	1708	102	3666	291	5897	577
A- Inorg	416	4	418	8	423	12	582	60	604	51	729	47	510	30	792	26	779	24
B- Inorg	428	15	422	15	435	25	631	71	600	99	772	51	535	22	778	47	717	49
A + F-Inorg	569	11	765	13	815	16	1095	65	1259	106	1842	169	1427	144	2404	315	2802	390
B + F-Inorg	558	7	884	31	1037	107	1308	151	1515	175	2119	222	1606	156	2611	321	3135	438
A + F	1307	4	1532	27	1873	211	2451	224	4242	577	7596	917	8630	122	107113	4414	120779	1720
B + F	1195	7	1792	97	2068	75	2866	245	5717	785	8002	449	8733	155	113585	443	125278	1462
Blk	457	9	460	13	464	14	592	39	541	39	580	48	431	25	689	37	664	69
Blk + F	472	16	789	171	890	170	1270	164	2047	292	3644	305	5317	969	96860	8155	114441	2565
F+ OA + FW	1015	8	14887	756	22374	202	29193	602	31718	539	51778	1071	53736	1010	70355	1336	70462	1270

Where; $\bar{x}$ is the mean CO_2 (ppm) of the triplicates produced in the microcosm headspace and SE is a standard error calculated from the triplicates.

A = leachate A, B= leachate B, F= filter, Blk= blank, Aut. F= autoclave filter, A-inorg = leachate A without inorganic amendments, B+F-Inorg= leachate B + Filter without inorganic amendment, F+Org+FW= microcosm containing filter, fresh water with organic amendments.

https://doi.org/10.5194/egusphere-2026-2864
Preprint. Discussion started: 4 June 2026

Appendix B: Mean CH_4 concentration and standard error of the triplicate measured in each microcosm headspace.

	Day(s)													
	1		5		9		23		54		580		810	
Sample ID	$\bar{x}CH_4 \pm$ SE (ppb)		$\bar{x}CH_4 \pm$ SE (ppb)		$\bar{x}CH_4 \pm$ SE (ppb)		$\bar{x}CH_4 \pm$ SE (ppb)		$\bar{x}CH_4 \pm$ SE (ppb)		$\bar{x}CH_4 \pm$ SE (ppb)		$\bar{x}CH_4 \pm$ SE (ppb)	
Air	3579	-	3565	-	3560	-	3188	-	3227	-	2936	-	3509	-
A	4616	376	4153	129	4120	122	7516	181	4934	49	3314	836	3145	119
B	3958	124	3897	130	4543	79	7027	257	5797	47	2373	24	3630	501
A + F	3856	66	3796	56	6147	47	6132	216	5298	439	5432	73	5661	227
B + F	3886	144	3808	120	5419	815	5830	135	5148	1056	5413	107	7775	1966
Blk	3892	181	3832	135	3641	69	3244	283	3879	196	2323	53	2127	16
Blk + F	4083	134	4225	286	7146	185	6847	44	5965	568	16211	4417	199413	21971
A + Aut.F	4265	441	4167	399	7117	137	6284	215	6275	38	4660	458	4873	1433
B + Aut.F	3781	2	3717	4	6545	37	5275	79	5349	111	4467	419	5599	28
A- Inorg	4170	230	4063	217	7754	184	7512	284	6164	1038	3274	923	3146	1057
B- Inorg	4140	71	4067	63	7702	59	7266	155	7235	30	2930	635	2735	648
A + F-Inorg	3906	123	3838	111	7098	238	6839	177	7215	130	3887	84	3866	106
B + F-Inorg	3808	40	3755	14	6824	529	4657	1082	6576	433	3919	62	3817	20
F+ OA + FW	3796	14	3720	13	5642	126	4375	91	5623	69	3906	62	3797	22

Where $\bar{x}$ is the mean CO_2 (ppm) of the triplicates produced in the microcosm headspace, and SE is a standard error calculated from the triplicates

7.0 Code and data availability

All data generated and analysed during this study, including DOM composition measurements, greenhouse gas (CO_2 and CH_4) incubation results, and LC-OCD outputs, are available from the corresponding author upon reasonable request. The analytical protocols and microcosm setup procedures are described in detail within the manuscript to ensure reproducibility. No proprietary code was used; all calculations and data processing were performed using standard laboratory software (ChromeCalc for LC-OCD integration and instrument-specific packages). In line with the Copernicus data policy, datasets supporting the findings of this study will be archived in an open repository and linked upon publication.

8.0 Author contribution

S/N	Author	Contribution
1	Muhammad Sabiu Jibrin	➢ Conceptualization ➢ Data curation ➢ Formal Analysis ➢ Funding Acquisition ➢ Methodology development ➢ Writing and reviewing
2	Abdulhamid Dahiru	➢ Contributed to conceptualisation ➢ Contributed to methodology design ➢ Data analysis ➢ Co in writing and reviewing

https://doi.org/10.5194/egusphere-2026-2864
Preprint. Discussion started: 4 June 2026

9.0 Competing interests:

The authors declare that they have no conflict of interest.

10.0 Statement on Inclusivity in Global Research

This research was conducted at the Lyell Centre, Heriot-Watt University, Scotland, using shale samples collected from the Tarfaya Basin, Morocco. We acknowledge the importance of international collaboration and the ethical responsibility of working with geological materials sourced from diverse regions. Our study was carried out with respect for the scientific and cultural contexts of both locations, aiming to generate insights that contribute to a globally inclusive understanding of subsurface carbon flux and microbial interactions relevant to geothermal energy systems.

11.0 Acknowledgements

The authors gratefully acknowledge the Petroleum Technology Development Fund (PTDF) for sponsoring this research. We extend our sincere thanks to the Lyell Centre, Heriot-Watt University, Scotland, where the study was conducted, for providing the facilities and support that made this work possible. Special appreciation goes to the Carbon Water Dynamics Group within the Centre for their valuable guidance, technical assistance, and collaborative spirit throughout the course of this project.

References

Ábel M., Judit M. S. and Maren B. (2021). Injection-related issues of a doublet system in a sandstone aquifer—a generalised concept to understand and avoid problem sources in geothermal systems. Geothermics. 2021; 97:102234. https://doi.org/10.1016/j.geothermics.2021.102234.

Aiken, G. R. (2002). "Organic matter in groundwater," in Proceedings of the U.S. Geological Survey Artificial Recharge Workshop, Sacramento, California, April 2–4, 2002, USGS Open-File Report 02-89, eds G. R. Aiken and E. L. Kuniansky (Denver, CO: U.S. Geological Survey).

Auffret, M. D., Karhu, K., Khachane, A., Dungait, J. A. J., Fraser, F., Hopkins, D. W. … Prosser, J. I. (2016). The Role of Microbial Community Composition in Controlling Soil Respiration Responses to Temperature. PLoS ONE, 11(10), 1–19. https://doi.org/10.1371/journal.pone.0165448

Aukes, P. J. K., Schiff, S. L., Venkiteswaran, J. J., Elgood, R. J. and Spoelstra J. (2021). Size-based characterisation of freshwater dissolved organic matter finds similarities within a waterbody type across different Canadian ecozones. Limnology and Oceanography Letters 6: 85–95, doi:10.1002/lol2.10180.31

Awoyemi, O. M., Achudume, A. C., and Okoya, A. A. (2014). The physicochemical quality of groundwater in relation to surface water pollution inMajidun area of Ikorodu, Lagos State,Nigeria. *American Journal Water Resource* **2**:126–133. doi: 10.12691/ajwr-2-5-4.

Billett, M. F. and Harvey, F. H. (2013): Measurements of CO2 and CH4 evasion from UK peatland headwater streams. In Biogeochemistry 114 (1-3), pp. 165–181. DOI: 10.1007/s10533-012-9798-9.

https://doi.org/10.5194/egusphere-2026-2864
Preprint. Discussion started: 4 June 2026

Brehme M, Nowak K, Abel M, Siklosi I, Willems C, Huenges E. (2020). Injection Triggered Occlusion of Flow Pathways in a Sedimentary Aquifer in Hungary. World Geothermal Congress 2020,

WGC 2020; Conference date: 21-05-2020. Through 26-05-2020; 2020. https://www.wgc2020.com/

Catalán N, Ortega SH, Gröntoft H, Hilmarsson TG, Bertilsson S, Wu P, Levanoni O, Bishop K, Bravo AG (2017). Effects of beaver impoundments on dissolved organic matter quality and biodegradability in boreal riverine systems. Hydrobiologia 793:135–148. https://doi.org/10.1007/s10750-016-2766-y.

Colwell, F.S. and D'Hondt, S. (2013). Nature and Extent of the Deep Biosphere. Reviews in Mineralogy and Geochemistry 75: 547–574.

Davidson, E. A., and Janssens, I. A. (2006). Temperature sensitivity of soil carbon decomposition and feedbacks to climate change. *Nature,* **440**:165–173. doi: 10.1038/nature04514.

Ding, J. J., Zhang, Y. G., Wang, M. M., Sun, X., Cong, J., Deng, Y., et al. (2015). Soil organic matter quantity and quality shape microbial community compositions of subtropical broadleaved forests. *Molecular Ecology*, **24**:5175–5185. doi: 10.1111/mec.13384.

Dinsmore, K. J. and Billett, M. F. (2008): Continuous measurement and modeling of CO2 losses from a peatland stream during stormflow events. In Water Resources Research 44 (12). DOI:10.1029/2008wr007284.

Dinsmore, K. J., Billett, M. F., SKIBA, U. M.T.E., Rees, R. M., Drewer, J. and Helfter, C. (2010): Role of the aquatic pathway in the carbon and greenhouse gas budgets of a peatland catchment. In Global change biology 16 (10), pp. 2750–2762. DOI: 10.1111/j.1365-2486.2009.02119.x.

Dinsmore, K. J., Wallin, M. B., Johnson, M. S., Billett, M. F., Bishop, K., Pumpanen, J. and Ojala, A. (2013): Contrasting CO2 concentration discharge dynamics in headwater streams. A multicatchment comparison. In J. Geophys. Res. Biogeosci. 118 (2), pp. 445–461. DOI:10.1002/jgrg.20047.

Drewer, J., Lohila, A., Aurela, M., Laurila, T., Minkkinen, K. and Penttilä, T. et al. (2010): Comparison of greenhouse gas fluxes and nitrogen budgets from an ombotrophic bog in Scotland and a minerotrophic sedge fen in Finland. In European Journal of Soil Science 61 (5), pp. 640–650. DOI: 10.1111/j.1365-2389.2010.01267.x.

Duc, N. T. (2010). Abiotic and biotic methane dynamics in relation to the origin of life. A Dissertation for the degree of Doctor of Philosophy in Natural Science, Department of Geological Sciences, Stockholm University, SE-106 91 Stockholm, Sweden.

European Commission. (2020). CORDIS Results Pack on Geothermal Energy: A new and viable alternative energy source to help achieve Europe's climate ambitions. Publications Office of the European Union. ISSN: 2599-8293. ISBN: 978-92-78-42157-1. doi:10.2861/430671.

Findlay, S.E.G. and Parr, T. B. (2017). Dissolved organic matter. Methods in Stream Ecology, 24: 21-36, http://dx.doi.org/10.1016/B978-0-12-813047-6.00002-4.

Goodwin, C. R., Covington, B. C., Derewacz, D. K., McNees, C. R., Wikswo, J. P., McLean, J. A., et al. (2015). Structuring microbial metabolic responses to multiplexed stimuli via

https://doi.org/10.5194/egusphere-2026-2864
Preprint. Discussion started: 4 June 2026

self-organising metabolomics maps. Chem. Biol. 22, 661–670. doi: 10.1016/j.chembiol.2015.03.020.32

Heimann, M., and Reichstein, M. (2008). Terrestrial ecosystem carbon dynamics and climate feedbacks. *Nature,* **451**: 289–292. doi: 10.1038/nature06591

HM Government (2021). Net Zero Strategy: Build Back Greener. Available from: https://assets.publishing.service.gov.uk/government/uploads/system/uploads/attachment_data/file/1033990/net-zero-strategybeis.pdf.

Horstmann, L. (2018). Pilot investigation of the potential of source rock leachates to stimulate microbial organic carbon degradation; Methodological procedure. ERASMUS internship, pp. 2- 8.

Huber, S.A., Balz, A., Abert, M., Pronk, W. (2011). Characterization of aquatic humic and non-humic matter with size-exclusion chromatography – organic carbon detection – organic nitrogen detection (LC-OCD-OND).*Water Resource*, **45**:879–885.

Inagaki F, Motomura Y, Ogata S. (2003). Microbial silica deposition in geothermal hot waters. Appl Microbiol Biotechnol.2003;60(6):605–11. https:// doi. org/ 10. 1007/ s00253-002-1100-y.

Jiao, N., Herndl, G. J., Hansell, D. A., Benner, R., Kattner, G., Wilhelm, S. W., et al. (2010). Microbial production of recalcitrant dissolved organic matter: long-term carbon storage in the global ocean. *Nature Reviews Microbiology,* **8**:593–599. doi: 10.1038/nrmicro2386.

Ji, X., Tiraferri, A., Zhang, X., Liu, P., Gan, Z., Crittenden, J. C., Ma, J., & Liu, B. (2023). Dissolved organic matter in complex shale gas wastewater analyzed with ESI FT-ICR MS: Typical characteristics and potential of biological treatment. Journal of Hazardous Materials, 447, 130823. https://doi.org/10.1016/j.jhazmat.2023.130823

Kadnikov, V. V., Mardanov, A. V., Beletsky, A. V., Karnachuk, O. V. and Ravin, N. V. (2020). Microbial life in the deep subsurface aquifer illuminated by metagenomics. Frontiers in microbiology, Volume **11**: 572252, doi: 10.3389/fmicb.2020.572252.

Kallenbach, C. M., Frey, S. D., and Grandy, A. S. (2016). Direct evidence for microbial-derived soil organic matter formation and its ecophysiological controls. *Nature Communications*, **7**:13630.doi: 10.1038/ncomms13630

Kelleher, B. P., and Simpson, A. J. (2006). Humic substances in soils: are they chemically distinct? *Environmental Science Technology*, **40:** 4605–4611. doi: 10.1021/es0608085.

Kellerman, A. M., T. Dittmar, D. N. Kothawala, and L. J. Tranvik. (2014). Chemodiversity of dissolved organic matter in lakes driven by climate and hydrology. Nat. Commun. 5: 1–8. doi:10.1038/ncomms4804.

Koch, B. P., Kattner, G., Witt, M., and Passow, U. (2014). Molecular insights into the microbial formation of marine dissolved organic matter: recalcitrant or labile? *Biogeosciences* **11**:4173–4190. doi: 10.5194/bg-11-4173-2014.

Kogel-Knabner, I. (2002). The macromolecular organic composition of plant and microbial residues as inputs to soil organic matter. *Soil Biology and Biochemistry*, **34**:139–162. doi:10.1016/S0038-0717(01)00158-4.

https://doi.org/10.5194/egusphere-2026-2864
Preprint. Discussion started: 4 June 2026

Kolonic, S., Sinninghe Damsté, J.S., Böttcher, M.E., Kuypers, M.M.M. Kuhnt, W., Beckmann, B., Scheeder, G. and Wagner, T. (2002). Geochemical characterization of Cenomanian/Turonian black shales from the Tarfaya basin (sw morocco); relationships between Palaeoenvironmental conditions and early sulphurization of sedimentary organic matter. *Journal of Petroleum Geology*, 25 (**3**):325-350.

Kuhnt, W., Herbin, J.P., Thurow, J. and Wiedmann, J. (1990). Distribution of Cenomanian/Turonian organic facies in the western Mediterranean and along the adjacent Atlantic Margin. In: Huc, A.Y., (Eds.), Deposition of Organic Facies. AAPG Studies in Geology, 40, 133-160.

Kuhnt, W., Nederbragt, A. And Leine, L. (1997). Cyclicity of Cenomanian-Turonian organic-rich sediments in the Tarfaya Atlantic Coastal Basin (Morocco). Cretaceous Research, 18, 587-601.

Kye, H., Kim, K., Jung, Y., Abrha, Y. W., Nam, S. N., Choi, I. H., Kang, J. W. and Yoon, Y. (2021). Characterization of marine dissolved organic matter and its effect on ozonation. Chemosphere, 277:130332. doi: 10.1016/j.chemosphere.2021.130332.

Lin, X., T., faily, M. M., Green, S. J., Steinweg, J. M., Chanton, P., Imvittaya, A., et al. (2014). Microbial metabolic potential for carbon degradation and nutrient (nitrogen and phosphorus) acquisition in an Ombrotrophic Peatland. *Applied Environviromental Microbiology*, **80**:3531–3540. doi:10.1128/AEM.00206-14

McCarren, J., Becker, J. W., Repeta, D. J., Shi, Y., Young, C. R., Malmstrom, R. R., et al. (2010). Microbial community transcriptomes reveal microbes and metabolic pathways associated with dissolved organic matter turnover in the sea. *Proceedings of the National Academy of Sciences of the United States of America*, **107**: 16420–16427. doi:10.1073/pnas.1010732107.

Miles, R. A. and Doucette, W. J. (2001). Assessing the aerobic biodegradability of 14 hydrocarbons in two soils using a simple microcosm/respiration method. *Chemosphere*, **45**(2001): 1085- 1090.34

Moore, E. K., Caldwell Eldridge, S. L., Tomaszewski, E. J., Varonka, M. S., Martini, A. M., Carley, M., Schramski, J., Zheng, H., & Barnhart, E. P. (2025). Metaproteomics and metagenomics reveal microbial pathways of organic matter degradation and methanogenesis in a marginally producing natural gas well. Communications Earth & Environment, 6(1), 873. https://doi.org/10.1038/s43247-025-02776-2

Mouser, P. J., Liu, S. and Cluff, M. A. (2016). Redox conditions alter biodegradation rates and microbial community dynamics of hydraulic fracturing fluid organic additives in soil-groundwater microcosms. *Environmental Engineering Science*, 33(**10**):827-838.

Okland, I., Huang, S., Thorseth, I. H., and Pedersen, R. B. (2014). Formation of H2, CH4 and N-species during low-temperature experimental alteration of ultramafic rocks. Chemical Geology, 387, 22-34.

Osburn, M. R., Casar, C. P., Kruger, B., Momper, L., Flynn, T. M. and Amend, J. P. (2020). Contrasting Variable and Stable Subsurface Microbial Populations: an ecological time series analysis from the Deep Mine Microbial Observatory, South Dakota, USA, bioRxiv preprint, https://doi.org/10.1101/2020.09.15.298141.

https://doi.org/10.5194/egusphere-2026-2864
Preprint. Discussion started: 4 June 2026

Osterholz, H., Niggemann, J., Giebel, H. A., Simon, M., and Dittmar, T. (2015). Inefficient microbial production of refractory dissolved organic matter in the ocean. *Nature Communications,* **6**:7422. doi: 10.1038/ncomms8422

Ren, H., Chen, S., Shang, J. et al. Insights into the Response and Evolution of Microbial Communities During Long-Term Natural Remediation of Contaminated Abandoned Shale Gas Wells. Water Air Soil Pollut 235, 729 (2024). https://doi.org/10.1007/s11270-024-07545-z

Saini, R., Kapoor, R., Kumar, R., Siddiqi, T. O. and Kumar, A. (2011). CO2 utilization microbes – A comprehensive review. Biotechnology advances, 29(6): 949 – 960.

Sand W. (2003). Microbial life in geothermal waters. Geothermics. 2003;32(4):655–67. https:// doi.org/ 10. 1016/ S0375-6505(03)00058-0 (Selected Papers from the European Geothermal Conference 2003).

Schlesinger, W. H., and Andrews, J. A. (2000). Soil respiration and the global carbon cycle. *Biogeochemistry,* **48**: 7–20. doi: 10.1023/A:1006247623877.

Siskin M. and Katritzky A.R. (1991). Reactivity of organic compounds in hot water: geochemical and technological implications. Science, 254(5029):231–7. https:// doi. org/ 10. 1126/ scien ce. 254. 5029. 231.

Spray, J. F., Wagner, T., Bischoff, J., Trojahn, S., Norouzi, S., Hill, W., Brasche, J., James, L., and Pereira, R. (2021): Unravelling Light and Microbial Activity as Drivers of Organic Matter Transformations in Tropical Headwater Rivers, *Biogeosciences*, https://doi.org/10.5194/bg-2021-92, 2021.35

Turnbull, L., Toyofuku, M., Hynen, A. L., Kurosawa, M., Pessi, G., Petty, N. K., et al. (2016). Explosive cell lysis as a mechanism for the biogenesis of bacterial membrane vesicles and biofilms. Nat.Commun. 7:11220. doi: 10.1038/ncomms11220.

Wani, A. K., Akhtar, N., Sher, F., Navarrete, A. A. and Américo-Pinheiro, J. H. P. (2022). Microbial adaptation to different environmental conditions: molecular perspective of evolved genetic and cellular systems. Archives of Microbiology, 204:144

Westphal A, Eichinger F, Eichinger L, Würdemann H. (2019). Change in the microbial community of saline geothermal fluids amended with a scaling inhibitor: effects of heat extraction and nitrate dosage. Extremophiles. 2019;23(3):283–304. https:// doi. org/ 10. 1007/ s00792-019-01080-0.

Widdel, F. and Bak. F. (1992). Gram-negative mesophilic sulfate-reducing bacteria A. Balows, H. G. Trüper, M. Dworkin, W. Harder, and K.-H. Schleifer. The Prokaryotes, 2nd ed Springer-Verlag New York, **3**:3352–3378.

Widdel, F., Kohring, G. W. and Mayer, F. (1983). Studies on dissimilatory sulfate-reducing bacteria that decompose fatty acids. Arch. Microbiol. 134, 286–294. https://doi.org/10.1007/BF00407804

Wiegner, T. N., and Seitzinger, S. P. (2004). Seasonal bioavailability of dissolved organic carbon and nitrogen from pristine and polluted freshwater wetlands. *Limnology and Oceanography*, **49**:1703–1712. doi:10.4319/lo.2004.49.5.1703.

Wilke, F. D.H., Vieth-Hillebrand, A., Naumann, R. and Jörg Erzinger, B. H. (2015) "Induced mobility of inorganic and organic solutes from black shales using water extraction: Implications for shale gas exploitation" Applied Geochemistry, 63 (2015): 158-168.

https://doi.org/10.5194/egusphere-2026-2864
Preprint. Discussion started: 4 June 2026

Wu X, Wu L, Liu Y, Zhang P, Li Q, Zhou J, Hess NJ, Hazen TC, Yang W and Chakraborty R (2018). Microbial Interactions with Dissolved Organic Matter Drive Carbon Dynamics and Community Succession. Front. Microbiol. 9:1234. doi: 10.3389/fmicb.2018.01234

Wu, L., Wen, C., Qin, Y., Yin, H., Tu, Q., Van Nostrand, J. D., et al. (2015). Phasing amplicon sequencing on Illumina Miseq for robust environmental microbial community analysis. *BMC Microbiology*, **15**:125. doi: 10.1186/s12866-015-0450-4.

Yates, C.A., Johnes, P.J., Owen, A.T., Brailsford, F.L., Glanville, H.C., Evans, C.D., Marshall, M.R., Jones, D.L., Lloyd, C.E.M., Jickells, T. and Evershed R.P. (2019). Variation in dissolved organic matter (DOM) stoichiometry in U.K. freshwaters: assessing the influence of land cover and soil C: N ratio on DOM composition Limnol. Oceanogr. 64 (6) (2019), pp. 2328-2340.

Young, K. C.,Maurice, P. A., Docherty, K. M., and Bridgham, S. D. (2004). Bacterial degradation of dissolved organic matter from two northern Michigan streams. *Geomicrobiology Journal, 21*:521–528. doi:10.1111/j.1462-2920.2010.02176.x 36

Zhang, P., Wu, W., Van Nostrand, J. D., Deng, Y., He, Z., Gihring, T., et al. (2015). Dynamic succession of groundwater functional microbial communities in response to emulsified vegetable oil amendment during sustained in situ U (VI) reduction. *Applied Environmental Microbiology,*81, 4164–4172. doi:10.1128/AEM.00043-15

Zhu, K., Yuan, M., Shi, Z., Qin, Y., Deng, Y., Cheng, L., et al. (2016). Tundra soil carbon is vulnerable to rapid microbial decomposition under climate warming. Nat. Clim. Chang 6, 595–600. doi:10.1038/ismej.2017.75

Zhu, Y., Vieth-Hillebrand, A., Wilke, F. D. H. and Horsfield, B. (2015). Characterization of watersoluble organic compounds released from black shales and coals. *International Journal of Coal Geology*, **150-151** (2015): 265-275.